Earth System
Dynamics
Discussions

Evaluation of terrestrial pan-Arctic carbon cycling using a data-assimilation system

Efrén López-Blanco[1,2], Jean-François Exbrayat[2,3], Magnus Lund[1], Torben R. Christensen[1,4], Mikkel P. Tamstorf[1], Darren Slevin[2], Gustaf Hugelius[5], Anthony A. Bloom[6], Mathew Williams[2,3]

[1] Department of Biosciences, Arctic Research Center, Aarhus University, Frederiksborgvej 399, 4000 Roskilde, Denmark
[2] School of GeoSciences, University of Edinburgh, Edinburgh, EH93FF, UK
[3] National Centre for Earth Observation, University of Edinburgh, Edinburgh, EH9 3FF, UK
[4] Department of Physical Geography and Ecosystem Science, Lund University, Sölvegatan 12, 223 62 Lund, Sweden
[5] Department of Physical Geography and Bolin Centre for Climate Research, Stockholm University, 106 91 Stockholm, Sweden
[6] Jet Propulsion Laboratory, California Institute of Technology, Pasadena, CA 91109, USA

Correspondence to: Efrén López-Blanco (elb@bios.au.dk)

Keywords: Arctic tundra, Arctic taiga, Net Ecosystem Exchange, Gross primary production, Ecosystem Respiration, carbon stocks, transit times, field observations, global vegetation models.

Abstract. There is a significant knowledge gap in the current state of the terrestrial carbon (C) budget. The Arctic accounts for approximately 50% of the global soil organic C stock, emphasizing the important role of Arctic regions in the global C cycle. Recent studies have pointed to the poor understanding of C pools turnover, although remain unclear as to whether productivity or biomass dominate the biases. Here, we use an improved version of the CARDAMOM data-assimilation system, to produce pan-Arctic terrestrial C-related variables without using traditional plant functional type or steady-state assumptions. Our approach integrates a range of data (soil organic C, leaf area index, biomass, and climate) to determine the most likely state of the high latitude C cycle at a 1° x 1° resolution for the first 15 years of the 21st century, but also to provide general guidance about the controlling biases in the turnover dynamics. As average, CARDAMOM estimates 513 (456, 579), 245 (208, 290) and 204 (109, 427) g C m^{-2} yr^{-1} (90% confidence interval) from photosynthesis, autotrophic and heterotrophic respiration respectively, suggesting that the pan-Arctic region acted as a likely sink -55 (-152, 157) g C m^{-2} yr^{-1}, weaker in tundra and stronger in taiga, but our confidence intervals remain large (and so the region could be a source of C). In general, we find a good agreement between CARDAMOM and different sources of assimilated and independent data at both pan-Arctic and local scale. Using CARDAMOM as a benchmarking tool for global vegetation models (GVM), we also conclude that turnover time of vegetation C is weakly simulated in vegetation models and is a major component of error in their forecasts. Our findings highlight that GVM modellers need to focus on the vegetation C stocks dynamics, but also their respiratory losses, to improve our process-based understanding of internal C cycle dynamics in the Arctic.

1 Introduction

Arctic ecosystems play a significant role in the global carbon (C) cycle (Hobbie et al., 2000; McGuire et al., 2009; McGuire et al., 2012; van der Molen et al., 2007). Slow organic matter decomposition rates due to cold and poorly drained soils in combination with cryogenic soil processes have led to an accumulation of large stocks of C stored in the soils, much

35 of which is currently held in permafrost (Tarnocai et al., 2009). The permafrost region soil organic C (SOC) stock is more than twice the size of the atmospheric C stock; and accounts for approximately half of the global soil organic C stock (Hugelius et al., 2014; Jackson et al., 2017). High latitude ecosystems are experiencing a warming increase that is nearly twice the global average (AMAP, 2017). SOC mineralisation may increase rapidly in response to warming, which may lead to an increase in release of carbon dioxide (CO_2) through heterotrophic respiration (Schuur et al., 2015) and thus increased emissions of CO_2

40 through ecosystem respiration (R_{eco}). However, temperature-induced vegetation changes (Lucht et al., 2002; Zhou et al., 2001) may mitigate those effects by photosynthetic enhancement (Abbott et al., 2016; Myers-Smith et al., 2015; Myneni et al., 1997). Consequently, phenology shifts may feedback on climate with unclear magnitude and sign (Anav et al., 2013; Murray-Tortarolo et al., 2013; Peñuelas et al., 2009). As a result of the significant changes that are already affecting the structure and function of Arctic ecosystems, it is critical to understand and quantify the C dynamics of the terrestrial tundra and taiga and

45 their responses to climate change (McGuire et al., 2012).

Despite the importance of Arctic tundra and taiga biomes in the global C cycle, our understanding of controls interacting between C storage and turnover is deficient (Hobbie et al., 2000). There are large gaps of knowledge in the current state of the pan-arctic terrestrial C budget that is mainly due to the vast uncertainties in C allocation, C stocks and transit times at global scales (Bloom et al., 2016; Carvalhais et al., 2014; Friend et al., 2014). At local scale, the net ecosystem exchange

50 (NEE) of CO_2 between the land surface and the atmosphere is usually measured using eddy covariance EC techniques (Baldocchi, 2003). International efforts have led to the creation of global networks such as FLUXNET (http://fluxnet.fluxdata.org/) and ICOS (https://www.icos-ri.eu/), to harmonise data and support the reduction of uncertainties around the C cycle and its driving mechanisms. However, upscaling field observations to estimate regional to global C budget presents important challenges due to insufficient spatial coverage of measurements and heterogeneous landscape mosaics

55 (McGuire et al., 2012). Furthermore, harsh environmental conditions in high latitude ecosystems and their remoteness complicates the collection of high quality data (Grøndahl et al., 2008; Lafleur et al., 2012). Given the lack of continuous, spatially distributed ground-based scale observations of NEE in the Arctic, it remains a challenging task to calculate with certainty whether or not the Arctic is a net C sink or a net C source, and how the net C balance will evolve in the future (Fisher et al., 2014).

60 Beyond direct ground observations, C cycle modelling in process-based global vegetation models (GVMs) typically relies on pre-arranged parameters retrieved from literature, prescribed plant-functional-type (PFT) or spin-up processes until the C stocks (biomass and SOC) reach their steady state (Clark et al., 2011; Friend and White, 2000; Ito and Inatomi, 2012; Pavlick et al., 2013; Sitch et al., 2003; Smith et al., 2001; Woodward et al., 1995). Further, inherent differences of model structure contribute more significantly to GVM uncertainties (Exbrayat et al., 2018; Nishina et al., 2014), than from differences

65 in climate projections (Ahlström et al., 2012). Although the land surface is estimated to offset 30% of anthropogenic emissions of CO_2 (Canadell et al., 2007; Le Quéré et al., 2018), the terrestrial C cycle is currently the least constrained component of the global C budget (Bloom et al., 2016). Many model intercomparison projects have demonstrated a lack of coherence in future projections of terrestrial C cycling (Ahlström et al., 2012; Friedlingstein et al., 2014). Recently, many studies have used simulations from the first phase of the Inter-Sectoral Impact Model Intercomparison Project (ISIMIP) (Warszawski et al.,

70 2014) to evaluate the importance of key elements regulating vegetation C dynamics, but also the estimated magnitude of their associated uncertainties (Exbrayat et al., 2018; Friend et al., 2014; Nishina et al., 2014; Nishina et al., 2015; Thurner et al., 2017). For example, the interactions between the land C cycling and climate is primarily determined by C turnover and productivity (Carvalhais et al., 2014). However, the spatial variability with climate has been more studied for NPP than for C

Earth System
Dynamics
Discussions

turnover processes (Thurner et al., 2017). Global scale vegetation model development has intensely concentrated on ecosystem productivity whereas the dynamics of C turnover, here addressed as transit time (Ceballos-Núñez et al., 2017; Sierra et al., 2017), has been less studied (Friend et al., 2014). Friend et al., 2014 detailed that transit time dominates uncertainty in terrestrial vegetation responses to future climate and atmospheric CO_2. They found a 30% larger variation in modelled vegetation C change than response of NPP. Nishina et al. (2015) also suggested that long term C dynamics within ecosystems (vegetation turnover and soil decomposition) are more critical factors than photosynthetic processes (i.e. GPP or NPP). The respective contribution of bias from biomass and NPP to biases in transit times remain unquantified. Without an appropriate understanding of current state of basic components of the C cycle, the understanding of C cycle feedbacks to climate change remains highly uncertain (Hobbie et al., 2000; Koven et al., 2015a).

Over the past decade, an increasing number of datasets has improved our understanding of the terrestrial C dynamics, including global scale vegetation dynamics. These range from machine-learning based upscaling of FLUXNET data, remotely-sensed biomass products or the creation of a harmonized soil databases. Despite the increasing volume of C-cycling related products, they do not provide estimates of the internal dynamics which regulate the C cycle and its response to changes. An approach to circumvent these issues is to integrate models and data to estimate these dynamics in agreement with observations. Here, we use the CARbon DAta MOdel framework (CARDAMOM) (Bloom et al., 2016; Smallman et al., 2017) to retrieve the pan-Arctic terrestrial carbon cycle for the 2000-2015 period in agreement with gridded observations of LAI, biomass and SOC stocks.

In this paper, we compare analyses of C dynamics of Arctic tundra and taiga for the period 2000-2015 for (a) global products of GPP (Jung et al., 2017; Tramontana et al., 2017) and heterotrophic respiration (R_h) (Hashimoto et al., 2015); (b) NEE, GPP and R_{eco} field observations from 8 sub- and high- Arctic sites included in the FLUXNET2015 dataset (Belelli Marchesini et al., 2007; Bond-Lamberty et al., 2004; Goulden et al., 1996; Ikawa et al., 2015; Kutzbach et al., 2007; López-Blanco et al., 2017; Lund et al., 2012; Sari et al., 2017), and (c) 6 GVM (HYBRID, JeDi, JULES, LPJmL, SDGVM and VISIT) from the ISI-MIP comparison project (Warszawski et al., 2014). Our objectives are (1) to present and evaluate the retrievals and uncertainties of the current state of the pan-Arctic terrestrial C cycling using a model-data fusion system, (2) to quantify the degree of agreement between our better constrained product with several sources of data available, from local to global scale, and (3) to use CARDAMOM as a benchmarking tool for the ISIMIP models to provide general guidance towards GVM improvements. Finally, we suggest future work to be done in the context of pan-Arctic C cyling modelling at the global scale.

2 Data and methods

2.1 Pan-Arctic region

The spatial domain we considered in this study (Figure S1) corresponds to the extent of the Northern Circumpolar Soil Carbon Database version 2 (NCSCDv2) dataset (Hugelius et al., 2013a; Hugelius et al., 2013b), bounded by latitudes 44°N - 80°N and longitudes 180°W - 180°E, and at a spatial resolution of 1° x 1°. This area of study totals 18.7 million km^2 of land area. We used the GlobCover vegetation map product developed by the European Space Agency (Bontemps et al., 2011) to separate regions dominated by non-forested and forested land cover types (hereafter referred as tundra and taiga, respectively) (Figure S1). The differentiation between tundra and taiga grid cells is in agreement with the tree line delimitated by Brown et al. (1997) together with the tundra domain defined from the Regional Carbon Cycle Assessment and Processes (RECCAP) Activity reported by McGuire et al. (2012). However, the tundra region extents into taiga regions without presence of trees in some areas such as the extensive grasslands in South Russia and Mongolia (Figure S1). This classification of tundra and taiga totals 9.0 and 9.7 million km^2 of land area, respectively.

Earth System
Dynamics
Discussions

2.2 The CARbon DAta MOdel framework

Here we use the CARbon DAta MOdel framework (CARDAMOM; Bloom et al., 2016) to retrieve terrestrial C cycle

115 dynamics, including explicit confidence intervals, in the pan-Arctic region. CARDAMOM is centred around the Data
Assimilation Linked Ecosystem Carbon version 2 (DALEC2), to simulate land-atmosphere C fluxes and the evolution of six
C stocks (foliage, labile, wood, roots, soil organic matter (SOM) and surface litter) and corresponding fluxes (Bloom and
Williams, 2015; Williams et al., 2005). DALEC2 includes 17 parameters controlling the processes of plant phenology,
photosynthesis, allocation of primary production to respiration and vegetation carbon stocks, plant and organic matter turnover

120 rates, all established within specific prior ranges based on ecologically viable limits (Table S1). DALEC2 simulates GPP and
its allocation to the four plant stocks and autotrophic respiration (R_a) as time-invariant fraction. Plant C decays into litter and
soil stocks where microbial decomposition generates heterotrophic respiration (R_h). In each plant, litter and soil stock turnover
is simulated using temperature dependent first-order kinetics. The Net Ecosystem Exchange (NEE) is calculated as the
difference between GPP and the sum of the respiration fluxes ($R_{eco} = R_a + R_h$), while Net Primary Productivity (NPP) is the

125 difference between GPP and R_a.

CARDAMOM is driven by climate data from the European Centre for Medium-Range Weather Forecast (ECMWF)
Reanalysis interim (ERA-interim) dataset (Dee et al., 2011) for the 2000-2015 period. A Bayesian Metropolis-Hastings
Markov chain Monte Carlo (MHMCMC) algorithm is used to retrieve the posterior distribution of 17 process parameters
according to observational constraints and Ecological and Dynamic constraints (EDCs; Bloom and Williams, 2015). EDCs

130 ensure that DALEC2 simulates the terrestrial carbon cycle in agreement with ecological theory. Observational constraints
include monthly time series of Leaf Area Index (LAI) from the MOD15A2 product (Myneni et al., 2002), estimates of
vegetation biomass and soil organic carbon content. In this paper, there are two main differences with the global approach
described in Bloom et al. (2016). First, the biomass constraints used by Bloom et al. (2016) only cover tropical regions. Instead,
here we use global biomass estimates from Carvalhais et al. (2014) which are based on remotely-sensed forest biomass

135 (Thurner et al., 2014) and upscaled GPP based on data driven estimates (Jung et al., 2011) covering the pan-Arctic domain.
Second, we constrained the storage of soil organic carbon (SOC) in the 0-1 m topsoil from the Circum-Arctic permafrost
region (Brown et al., 1997) using the NCSCD spatial explicit product (Hugelius et al., 2013a; Hugelius et al., 2013b) instead
of the Harmonized World Soil Database (HWSD) (FAO/IIASA/ISRIC/ISSCAS/JRC, 2012). While we report results using
this configuration, we provide estimates of the sensitivity of retrievals to the choice of SOC database and the inclusion or

140 omission of C_{veg} prior (global biomass product) in the Supplement.

We apply the setup described above to 3433 1° x 1° pixels (1815 in tundra; 1618 in taiga) using a monthly time step.
Each pixel is treated independently without assuming a prior land cover type. Prior values for two parameters (fraction of GPP
respired and canopy efficiency) are set according to Bloom et al. (2016). The MHMCMC is performed three times until
convergence and a total of 1500 parameter sets is sampled from the posterior distribution of parameter sets which allow

145 producing corresponding density function of all C fluxes and stocks. In the following we report highest confidence results
(median; P50) and the uncertainty represented by the 90% confidence interval (5th percentile to 95th percencile, $\binom{P95}{P05}$). We
aggregated the different C stocks into photosynthetic (C_{photo}), vegetation (C_{veg}) and soil (C_{dom}) C stocks. In this study, we
addressed C turnover rates and decomposition processes as their inverse rates, this is the C transit time (TT_{photo}, TT_{veg} and
TT_{dom}), represented as the ratio between each C stock and NPP. Transit time is an important diagnostic metric that is

150 independent of model internal structure, and good candidate to compare among models.

2.3 Model evaluation at local and and pan-Arctic scales

At the pan-Arctic scale, we compared our CARDAMOM GPP with FLUXCOM data from Jung et al. (2017).
155 FLUXCOM is based on a machine-learning approach to upscale local GPP data from eddy-covariance towers and provide gridded estimates of monthly fluxes at 0.5º x 0.5º resolution. FLUXCOM has been used in previous studies as a benchmark for simulated GPP (Exbrayat et al., 2018; Slevin et al., 2017). At a local scales, we compare CARDAMOM NEE and its partitioned components GPP and R_{eco} estimates against monthly aggregated values from the FLUXNET2015 dataset. We selected 8 sites located across sub- and high-Arctic latitudes, covering locations with different climatic conditions and
160 dominating ecotypes (Table S2). For this evaluation, we compared the same years for both observations and CARDAMOM, and we selected data using daytime method (Lasslop et al., 2010) due to the absence of true nighttime period during Arctic summers in some locations. Additionally, we selected variable u* threshold to identify insufficient turbulence wind conditions from year to year similar to López-Blanco et al. (2017). For readability purposes, in this data-model comparison we included the median (P50) ± the 50% confidence interval (percentile 25th to 75th; $\binom{P75}{P25}$) including both random and u* filtering
165 uncertainty following the method described in Papale et al. (2006). Some of the sites lack wintertime measurements and we filter out data for months with less than 10 % observations. Only NEE follows the standard micrometeorological sign convection presenting the uptake of C as negative (sink), and the release of C as positive (source); both GPP and R_{eco} are reported as positive fluxes.

2.4 Benchmark of Global Vegetation Models

170 We examined the pan-Arctic annual changes in net primary production (NPP), vegetation biomass carbon stocks (C_{veg}) and vegetation transit times (TT_{veg}; $TT_{veg} = C_{veg}/NPP$) using CARDAMOM as benchmark tool for six participating GVMs in the ISI-MIP comparison project (Warszawski et al., 2014). In this study we have considered HYBRID4 (Friend and White, 2000), JeDi (Pavlick et al., 2013), JULES (Clark et al., 2011), LPJml (Sitch et al., 2003), SDGVM (Woodward et al., 1995), and VISIT (Ito and Inatomi, 2012). The specific properties and degree of complexity of each ISI-MIP model are
175 summarized in Table S3, and more detailed information can be found in Friend et al. (2014) and Thurner et al. (2017).

In this study, each model simulation has been conducted under multiple General Circulation Models (GCM). Here we included HadGEM2-ES (Collins et al., 2011), IPSLCM5A-LR (Dufresne et al., 2013), MIROC-ESM-CHEM (Watanabe et al., 2011), GFDL-ESM2M (Dunne et al., 2012), and NorESM1-M (Bentsen et al., 2013) GCMs from the fifth phase of the Coupled Model Intercomparison Project (CMIP5) experiment (Arora et al., 2013; Taylor et al., 2012), which is temperature
180 and precipitation bias corrected following (Hempel et al., 2013). The comparisons with CARDAMOM for each GVM included the mean ensemble of all GCM forcings. The comparisons have been performed under the same spatial resolution as the CARDAMOM spatial resolution for the 2000-2004 period (1° x 1° resolution).

3 Results

The CARDAMOM framework quantified C fluxes, C stocks and transit times in plant, litter and soil carbon stocks
185 over the pan-Arctic land region (including the tundra and taiga partitioning) for the period 2000-2015 (Table 1). The system is likely a small C sink, although the 90% confidence intervals remain large (and so the region could be a source of C) (Table 1). Our analysis indicates that SOC is successfully assimilated (1:1 agreement), biomass stocks are 28% lower than earth observation mapping (Figure 1), and that GPP is 50% lower than FLUXCOM (Figure 2). We also suggest that R_h is lower in the tundra and higher in the taiga than upscaled estimates (Figure 2). We note that independent tests at EC locations suggests
190 that CARDAMOM's GPP is 30% biased high (Figure 3). This mismatch is important in the context of FLUXCOM, as noted (Figure 2). We benchmarked six GVMs to compare to not only their spatial variability across the pan-Arctic, tundra and taiga region (Figure 4), but also the degree of agreement between their mean model (6 GVMs – 5 GCMs) ensemble within the 90%

Earth System
Dynamics
Discussions

confidence interval of our framework (Figure 5, Table 3). We finally found that turnover time of vegetation C is weakly simulated in GVMs and is a major component of error in their forecasts (Figure 6).

3.1 Pan-Arctic retrievals of C cycle

Overall, we found that the pan-Arctic region (Table 1) acted as a consistent sink of C (area-weighted P50) over the 2000-2015 period with an average of -55.8 $\left(^{1158.1}_{-260.5}\right)$ g C m^{-2} yr^{-1}, P50 $\left(^{P95}_{P05}\right)$. However, tundra regions presented a weaker sink compared to taiga regions, this is -13.0 $\left(^{1107.7}_{-158.5}\right)$ and -104.1 $\left(^{1215.0}_{-375.4}\right)$ g C m^{-2} yr^{-1} respectively, but also lower uncertainties with nearly 1265.5 g C m^{-2} yr^{-1} between P05 and P95 in tundra. In general, the photosynthetic inputs exceeded the respiratory outputs (GPP > R$_{eco}$; Table 1), although the much larger uncertainties stemming from R$_{eco}$, and more specifically from R$_h$, compared with GPP complicate the net C sink/source estimate beyond the median's average ensembles. In the pan-Arctic region approximately half of GPP is autotrophically respired resulting in an NPP of 263.3 $\left(^{376.6}_{177.4}\right)$ g C m^{-2} yr^{-1}. Carbon use efficiency (NPP/GPP) averages 0.51$\left(^{0.55}_{0.46}\right)$, and marginally varied across tundra 0.50$\left(^{0.54}_{0.46}\right)$ and taiga 0.52$\left(^{0.56}_{0.46}\right)$. Despite these apparent small variations, tundra photosynthesized and respired (respectively 315.0$\left(^{450.1}_{226.9}\right)$ and 300.0$\left(^{1515.0}_{119.3}\right)$ g C m^{-2} yr^{-1}) approximately half as much as the Taiga region (736.5$\left(^{940.9}_{564.9}\right)$ and 618.98$\left(^{2106.3}_{276.6}\right)$ g C m^{-2} yr^{-1}).

The total size of the pan-Arctic vegetation C stock (C$_{veg}$) averaged 1.4$\left(^{6.0}_{0.5}\right)$ kg C m^{-2}, an estimate 94% smaller than the soil C stock (C$_{dom}$), 24.4$\left(^{47.6}_{10.3}\right)$ kg C m^{-2}. The soil C stock (fresh litter and soil organic matter, SOM) is clearly dominated by C$_{som}$, accounting for the 98.8%, which also dominates the terrestrial C stock in the pan-Arctic. Among the living C stocks, 91% of the C is allocated to the structural stocks (wood and roots; 1.3$\left(^{5.8}_{0.4}\right)$ kg C m^{-2}) compared to 9% to the photosynthetic stock (leaves and labile; 0.1$\left(^{0.1}_{0.1}\right)$ kg C m^{-2}). On average, the total ecosystem carbon density in the pan-Arctic region is 26.2$\left(^{51.1}_{11.7}\right)$ kg C m^{-2}, with slightly lower stocks in tundra (24.6$\left(^{50.7}_{10.8}\right)$ kg C m^{-2}) than taiga (28.0$\left(^{52.0}_{12.8}\right)$ kg C m^{-2}). In general, the taiga region accumulated on average ~44 %, ~55 % and ~10 % more C than tundra region in photosynthetic, structural and soil C stocks, respectively. In other words, taiga accumulates ~12 % more total C than tundra. Uncertainties in estimates of soil C stock are notably higher than for living C stocks, highlighting the lack of observational and mechanistic constraint on heterotrophic respiration.

The global mean C transit time is 1.4$\left(^{2.2}_{0.9}\right)$ years in leaves and labile plant tissue (TT$_{photo}$), 4.3 $\left(^{15.3}_{1.6}\right)$ years in stems and roots (TT$_{veg}$), and 129.3$\left(^{981.1}_{10.9}\right)$ years in litter and SOM (TT$_{dom}$). The total C transit time (TT$_{tot}$) (142.5$\left(^{1089.4}_{11.9}\right)$ years) is clearly dominated by the soil C stock, highlighting the very long periods of times that C particles can persist in Arctic soils. Interestingly, CARDAMOM estimates longer TT$_{veg}$ in Taiga compared to tundra with 5.9 $\left(^{8.6}_{3.2}\right)$ years vs 3.5 $\left(^{13.0}_{1.4}\right)$ years (for tundra), but also shorter transit times in TT$_{photo}$ and TT$_{dom}$ with 1.6 $\left(^{2.0}_{1.3}\right)$ and 157.3 $\left(^{329.9}_{63.1}\right)$ years respectively compared to 1.1 $\left(^{1.6}_{0.7}\right)$ years and 97.9 $\left(^{660.2}_{8.9}\right)$ years in tundra. The turnover rates estimated by CARDAMOM in tundra regions suggest a tendency towards longer transit times in the photosynthetic and soil C stocks, likely affected at some degree by low temperatures, wet soils, and thus slower decomposition processes.

Additionally, we performed a sensitivity analysis using four different experiments to assess the impact of using different soil C datasets (NCSCD and HWSD) and with-without biomass constraints (Table S4). These results show that the differences introduced by biomass constraints were significantly larger compared to the differences introduced by different soil C databases. Also, the difference between soil C databases resulted in shifts of 22% up to 20% in the total mean carbon stock (C$_{tot}$) and transit time (TT$_{tot}$). Our results showed significant (p < 0.01) differences whether biomass constraint was used in the framework or not. In simulations with biomass constraints, C$_{photo}$, C$_{veg,}$ and C$_{dom}$ stocks decreased the C stored ~ 78%, 62% and 10% respectively. Moreover, introducing biomass shortens retrievals the TT$_{photo}$ and TT$_{veg}$ by 87% and 60%, but also

Earth System
Dynamics
Discussions

their uncertainties (97.3% and 66% respectively). While using biomass constraints only has a negligible effect on productivity, increased respiration fluxes induce weaker C sink strengths.

3.2 Data assimilation and evaluation: from global to local scale

235 CARDAMOM retrieved the terrestrial C cycle in good agreement with priors of SOC and biomass. The agreement for SOC is a 1:1 relationship ($R^2 = 1.0$; RMSE = 0.97 kg C m^{-2}) while for biomass is close to 1:1 ($R^2 = 0.97$; RMSE = 0.46 kg C m^{-2}) (Figure 1). Using Carvalhais et al. (2014)'s biomass product led to a tendency towards larger accumulation (~28%) of C in the structural (wood and roots) stocks (Table S4) compared to the assimilated CARDAMOM's biomass. The understanding of ecological dynamics implemented in CARDAMOM cannot fully resolve Carvalhais et al. (2014) biomass in agreement with other products of LAI and SOC.

240 On the other hand, we compared our estimates of GPP and R_h with independent datasets to evaluate the model performance (Figure 2). We found GPP to be well correlated ($R^2 = 0.81$; RMSE = 0.43 kg C m^{-2}), but significantly lower (~51%) compared to Jung et al. (2017)'s GPP estimates. The areas with larger agreement, this is where FLUXCOM falls within CARDAMOM's 90% confidence interval, is in taiga regions, rather than in tundra (Figure 2). Also, we note evidence of a higher spatial variability in CARDAMOM (Figure 2). We found the R_h product from Hashimoto et al. (2015) is less

245 consistent with our estimates ($R^2 = 0.38$; RMSE = 0.09 kg C m^{-2}), with a tendency towards lower values in tundra pixels, and higher values in taiga pixels. R_h falls only within the 90% confidence interval of CARDAMOM in Central Northen Canada and Eurasia as well as the grasslands in South Russia and Mongolia. Moreover, the spatial variability is considerably smaller in Hashimoto et al. (2015)'s R_h, for example in central Eurasia. This confirms the uncetartanties previously noted in modelled respiratory processes (Table 1) where the upper P95 in R_h dominated NEE's uncertainties, but also the soil C stocks.

250 In order to get also a comparison with direct ground observations from the FLUXNET2015 dataset, we report here monthly aggregated P50 ± P25-75 estimates of NEE, GPP and R_{eco} to show timing and magnitudes, but also to diagnose whether CARDAMOM is in general agremment with flux tower data. Overall, CARDAMOM performed well in simulating observed NEE ($R^2 = 0.66$; RMSE = 0.51 g C m^{-2} month^{-1}; Bias = 0.16 g C m^{-2} month^{-1}), GPP ($R^2 = 0.85$; RMSE = 0.89 g C m^{-2} month^{-1}; Bias = 0.5 g C m^{-2} month^{-1}) and R_{eco} ($R^2 = 0.82$; RMSE = 0.63 g C m^{-2} month^{-1}; Bias = 0.35 g C m^{-2} month^{-1}) across

255 8 sub-Arctic and high-Arctic sites from the FLUXNET2015 dataset (Figure 3; Table 2). CARDAMOM NEE is 25% lower than FLUXNET2015, while GPP and R_{eco} are 30% and 10% higher, respectively. This mismatch is important in the context of the FLUXCOM GPP upscaling, as noted Some sites such as Hakasia, Samoylov, Poker Flat and Manitoba (NEE $R^2 = 0.85$, 0.87, 0.81, 0.7; GPP $R^2 = 0.98$, 0.98, 0.93, 0.93 and R_{eco} $R^2 = 0.98$, 0.89, 0.89, 0.80 respectively) represent better the seasonality and the magnitude of the C fluxes than the rest, i.e. Tiksi, Kobbefjord, Zackenberg and UCI-1998 (NEE $R^2 = 0.41$, 0.58, 0.54,

260 0.65; GPP $R^2 = 0.87$, 0.80, 0.84, 0.82 and R_{eco} $R^2 = 0.76$, 0.86, 0.86, 0.83 respectively). In general, CARDAMOM captured the beginning and the end of the growing season (Figure 3). However, the assimilation system showed bias due to difference in timing (earlier shifts of peak of the growing season in Manitoba and UCI-1998, GPP and R_{eco} or earlier end of the growing season in Poker Flat NEE) and differences in flux magnitudes (such as in Hakasia and GPP and R_{eco} and Kobbefjord NEE).

3.3 Benchmarking ISI-MIP with CARDAMOM

265 We used our highest confidence retrievals (i.e. median retrievals including LAI, biomass and soil organic C from NCSCD) to benchmark ISI-MIP's NPP, C_{veg} and TT_{veg} estimates. In Table 3 we quantified the degree of agreement and bias per assessed variable, spatial domain, and forward model. Overall, ISIMIP models are more in agreement with CARDAMOM's NPP estimates (for tundra and taiga respectively RMSE = 0.3 and 0.3 kg C m^{-2} yr^{-1}; Bias= 0.2 and 0.1 kg C m^{-2} yr^{-1}) than C_{veg} (RMSE = 2.4 and 2.8 kg C m^{-2}; Bias= 1.3 and 2.2 kg C m^{-2}) and TT_{veg} (RMSE = 19.0 and 6.1 years; Bias=

270 3.0 and 4.1 years). Also, the ISIMIP models consistently estimate larger median's mean NPP, C_{veg} and TT_{veg} than CARDAMOM (36%, 53% and 45% increase respectively) across the entire pan-Arctic domain (Figure 4 and 5). Interestingly,

Earth System
Dynamics
Discussions

HYBRID overestimated CARDAMOM's NPP and C_{veg} more clearly by 70% and 75%, but only 36 % for TT_{veg}. This is a representative example of compensating errors that may reduce the apparent bias in the inner dynamics. HYBRID TT_{veg} is the result of a systematic overestimation of NPP and C_{veg}. Overall, JEDI and SDGVM are the models in closer agreement with CARDAMOM (Table 3; Figure 4 and 5).

275

The separation between non-forested (tundra) and forested (taiga) areas also exposed some similarities and inconsistencies in model performance. For example, the ISIMIP models successfully assimilate the larger productivity, biomass and longer vegetation transit times in taiga compared to tundra (Figure 4). However, as average, the ISIMIP models are on average 56% more productive than CARDAMOM in tundra (0.16 vs 0.36 kg C m^{-2} yr^{-1} respectively), but only a 19% in taiga (0.39 vs 0.48 kg C m^{-2} yr^{-1}). Also, the tendency for C_{veg} and TT_{veg} coincide, estimating more biomass and transit times in tundra (55% and 46% respectively) than in taiga (51% and 44% respectively). In general, the overall agreement is closer for tundra than for taiga (Table 3).

280

For vegetation transit times, the pattern is more complex (Figures 4 and 5). The spatial variability patterns are similar to biomass, although larger (C_{veg} RMSE = 2.8 kg C m^{-2} and TT_{veg} RMSE = 4.3 kg C m^{-2}). We apportioned the error contribution to TT_{veg} by applying an attribution analysis. We used CARDAMOM to calculate hypothetical TT_{veg} estimates (i.e. calculate TT_{veg} with C_{veg} from CARDAMOM, and NPP from ISIMIP models, and with C_{veg} from ISIMIP models and NPP from CARDAMOM) to calculate the largest difference with CARDAMOM's reference TT_{veg}. We estimated the hypothetical TT_{veg} for each pixel in each model, and derived a pixel-wise measure of the contribution of biases in NPP and C_{veg} to biases in TT_{veg} by overlapping their distribution functions (Figure 6). The distribution of the differences relative to CARDAMOM revealed that the highest error (i.e. the lower overlapped area, and by extension the largest contributor to TT_{veg} biases) come from C_{veg} with only a 29% agreement in the distribution (Figure 6), while NPP agrees 76%.

285

290

4 Discussion

The CARDAMOM framework has been used to evaluate the terrestrial pan-Arctic C cycling in tundra and taiga at coarse spatio-temporal scale (at monthly and annual time steps for the 2000-2015 period and at 1° x 1° grid cells). The sensitivity analysis suggests that the C cycle retrieved by CARDAMOM is more sensitive to differences introduced by biomass constraints compared to the differences introduced by different soil C databases (Table S4). This result indicates that data on C stocks with shorter turnover (biomass) have a higher impact in the overall pan-Arctic dynamics than stocks with slower turnover (SOC). Overall, we found that the pan-Arctic region 1) was most likely a consistent sink of C (weaker in tundra and stronger in taiga), although the large uncertainties derived from respiratory processes (Table 1) strongly increase the 90% confidence interval uncertainty; 2) accumulated most of the C in the soil C stock (both fresh litter and SOM, but dominated by the latter with a contribution of about 97%); and 3) experienced longer transit times in leaves, labile, litter and SOM C stock located in tundra compared to taiga. In general, we found a good agreement between CARDAMOM and different sources of assimilated and independent data at both pan-Arctic and local scale. Finally, we used CARDAMOM as a benchmarking tool for six GVMs and we found that productivity processes are more in agreement with CARDAMOM than biomass, and thus biomass is the largest contributor to the bias influencing transit times. This finding suggest that there is a need to improve simulations of vegetation C stocks in Earth System models to get the inner dynamics right.

295

300

305

4.1. Pan-Arctic retrievals of C cycle

CARDAMOM retrievals are in good agreement with the SOC and biomass constraints (Figure 1). The simulation of SOC turnover is also weakly constrained - our analysis adjusts turnover time to match mapped stocks, hence the strong match of modelled to mapped SOC. So, independent data on SOC transit time (e.g. ^{14}C) data is required across the pan-Arctic region to provide stronger constraint on process parameters. Further, the retrievals presented here exhibited a coherent performance

310

Earth System
Dynamics
Discussions

of an independent global GPP product (Jung et al., 2017), but weaker agreement with an R_h product (Hashimoto et al., 2015)(Figure 2). Indeed, uncertainties in CARDAMOM R_h are substantially larger than for GPP, and that echoes in the large uncertainty found in NEE (Table 1). One difference between these two models is the lack of moisture limitation on respiration

315 in CARDAMOM. Conversely, GPP is relatively well-constrained through the assimilation of LAI and a prior for productivity (Bloom et al., 2016). An important mismatch has been found with regards GPP though. CARDAMOM GPP is 50% lower than FLUXCOM, but 30% higher than FLUXNET2015 EC data.

The agreement between earth observation data and EC data is surprisingly good given the vast scale difference. However, direct point-to-gridcell comparison with local observations derived from the FLUXNET2015 dataset (Figure 3,

320 Table 2) is challenging and always difficult. CARDAMOM outputs C stocks and fluxes in 1° x 1° grid cells, whereas local eddy covariance flux measurements are in the order of 1-10 hectares. Thus, for observational sites located in areas with complex terrain, such as Kobbefjord in coastal Greenland, the agreement can be expected to be low. For inland forest sites, such as Poker Flat in Alaska, there may be less differences in vegetation characteristics and local climatology between the local scale measurement footprint and the corresponding CARDAMOM grid cell. This scaling issue is likely to have a larger

325 impact on flux magnitudes compared with seasonal dynamics. In general, CARDAMOM captured the seasonal dynamics in NEE, GPP and R_{eco} well (Figure 3, Table 2). There was, however, a consistent timing-mismatch in early season flux increase, where CARDAMOM predicts earlier growing season onset compared with observations. This is likely due to the impact of snow cover, which is not explicitly included in the CARDAMOM framework.

At broader scales CARDAMOM estimates reported here are in good agreement with C flux observations and

330 estimates reported from McGuire et al. (2012) for the tundra domain, but also with the C stocks and transit times described by Carvalhais et al. (2014) in tundra and taiga, and the turnover rates (inverse of the transit times calculated here) supported by Thurner et al. (2017) in taiga regions. This performance compared to independently related C cycle components demonstrates that CARDAMOM is a robust and useful tool to assess large scale C cycle dynamics in the Arctic.

First, our NEE estimates reported in this study from Arctic tundra are inside the variability comparison of estimates

335 among field observation, regional process-based models, global-process based models and inversion models reported by McGuire et al. 2012. McGuire et al. 2012 reported that Arctic tundra was a sink of CO_2 of -150 Tg C yr^{-1} (SD=45.9) across the 2000-2006 period over an area of 9.16 x 10^6 km^2. Here CARDAMOM's NEE estimate for the same period estimated -125 Tg C yr^{-1} over an area of 9 x 10^6 km^2. For example, this exhaustive assessment of the C balance in Arctic tundra included approximately 250 estimates using the chamber and eddy covariance method from 120 published papers (McGuire et al., 2012;

340 Supplement 1) with an area-weighted mean of means estimate of -202 Tg C yr^{-1}. The regional applications reported by McGuire et al., 2012 estimated NEE in -187 Tg C yr^{-1}, including LPJ-Guess WHyMe (Smith et al., 2001), Orchidee (Koven et al., 2011), version 6 of the Terrestrial Ecosystem Model (TEM6) (McGuire et al., 2010) and the Terrestrial Carbon Flux (TCF) model (Kimball et al., 2009). These models also calculated GPP, NPP, R_a and R_h to be 350, 199, 151 and 182 g C $m^{-2}y^{-1}$, respectively. The DGVM applications included in McGuire et al., 2012 CLM4C (Lawrence et al., 2011), CLM4CN (Thornton et al., 2009),

345 Hyland (Levy et al., 2004), LPJ (Sitch et al., 2003), LPJ- Guess (Smith et al., 2001), O-CN (Zaehle and Friend, 2010), SDGVM (Woodward et al., 1995), and TRIFFID (Cox, 2001) estimated NEE in -93 Tg C yr^{-1} and GPP, NPP, R_a and R_h in 272, 162, 83 and 144 g C $m^{-2}yr^{-1}$ respectively. For the same period CARDAMOM has estimated the gross C fluxes in 318, 161, 154 and 148 g C m^{-2} yr^{-1} respectively.

Second, Carvalhais et al. (2014) estimated total ecosystem carbon (C_{tot}) of 20.5$\binom{52.5}{8.0}$ kg C m^{-2} for tundra and

350 24.8$\binom{58.0}{15.2}$ kg C m^{-2} for taiga, while CARDAMOM tundra was 24.6$\binom{33.0}{18.3}$ kg C m^{-2}, while 28.0$\binom{36.1}{21.5}$ kg C m^{-2} in taiga (Figure 4; Table 1). Therefore, Carvalhais et al. (2014)'s C_{tot} product stored only 16.8 and 11.5% less carbon in tundra and taiga respectively than CARDAMOM. Also, we noted that the numbers are in line with Carvalhais et al. (2014) thanks to the use of the biomass constraint dataset, where C_{photo}, C_{veg}, and C_{dom} stocks decreased the C stored ~ 78%, 62% and 10% respectively (Table S4). Overall, CARDAMOM estimated 20.3 and 5.7% longer transit times for tundra and taiga respectively, with average

Earth System
Dynamics
Discussions

355 values of $80.8\binom{195.2}{21.8}$ years in tundra and $51.2\binom{109.3}{22.1}$ years in taiga (CARDAMOM)(Table 1) compared to the $64.4\binom{259.8}{25.7}$ years
in tundra and $48.2\binom{111.6}{24.9}$ years in taiga in Carvalhais et al. (2014). These numbers have been retrieved from the same biome
classification and the confidence intervals include the 90% confidence interval of the calculated spatial variability. Both
datasets agree on the fact that high (cold) latitudes, first tundra, and second taiga have the longest transit times of the entire
globe (Bloom et al., 2016; Carvalhais et al., 2014).

360   Third, a recent study from Thurner et al. (2017) assessed temperate and taiga-related transit times, NPP and C_{veg}
taking into consideration the current poor process understanding of decomposition dynamics. Thurner et al 2017 used of 5-
year average NPP for the time period 2000-2004, applying both MODIS (Running et al., 2004; Zhao et al., 2005) and
BETHY/DLR (Tum et al., 2016) products. They use a biomass product (Thurner et al., 2014) at 0.5 degree while accounting
for both forest and non-forest vegetation. Our estimates of TT_{veg} for the exact same period are very close to Thurner et al.

365 (2017), where their $8.2\binom{11.5}{5.5}$ years using MODIS and $6.5\binom{8.7}{4.2}$ years using Bethy/DLR are close to the $5.2\binom{17.8}{1.9}$ years estimated
by our data assimilation approach. A note of caution here, the number reported by the authors are turnover rates, which are
inferred to transit times by just applying the inverse of turnover rates (TT_{veg}=1/turnover rates). Additionally, their estimated
NPP (0.35 (MODIS) and 0.45 kg C m^{-2} yr^{-1} (BETHY/DLR), without any uncertainty reported) is only 5% more productive as
average than CARDAMOM's NPP estimate of $0.4\binom{0.5}{0.3}$ kg C m^{-2} yr^{-1}; while the biomass derived from Thurner et al. (2014),

370 3.0 (±1.1) kg C m^{-2}, is 23% lower than our estimates of 2.3 $\binom{4.9}{1.2}$ kg C m^{-2} for the same period and for the taiga region. Again,
here, the presence of biomass as data constraint has helped to decrease TT_{veg} and its uncertainty significantly.

4.2. CARDAMOM as a benchmarking tool

        The CARDAMOM framework has proven capable of effectively simulating Arctic C cycling dynamics in the entire
pan-Arctic region, but also to partition it in its two main biomes, i.e. tundra and taiga (Table 1, Figure 1, 2, 3, Discussion 4.1).

375 Recent studies used the same GVM inter-comparison models we used here raising strong arguments about the differences in
model formulations and their impact on calculations, significant uncertainties and poor representation of C stocks dynamics at
global scale (Exbrayat et al., 2018; Friend et al., 2014; Nishina et al., 2014; Nishina et al., 2015; Thurner et al., 2017). Here,
we have a considerably more data-constrained and data-integrated approach than GVMs to calculate C dynamics.
Consequently, CARDAMOM is a good candidate to use as benchmark to pinpoint caveats of model performance. For example,

380 Exbrayat et al. (2018) found that ISIMIP models are less in agreement for NPP in boreal latitudes compared to global
CARDAMOM retrievals (Bloom et al., 2016) that did not include biomass constraints in boreal regions. In this study, we
incorporated two new layers of data constraints suitable for high latitudes (Carvalhais et al., 2014; Hugelius et al., 2013b)
compared to their version of CARDAMOM, and we found that NPP had one of the best agreements among the assessed
variables (compared to C_{veg} and TT_{veg}), but also slightly better performance in tundra than taiga (Bias = 9 and 19 g C m^{-2} yr^{-1}

385 respectively) (Figure 4 and 5; Table 3).

        Also, recent studies have emphasized the significance of model comparison of turnover rates/ transit times (Ceballos-
Núñez et al., 2017; Sierra et al., 2017), as diagnostic metrics independent of model internal structure. From a modelling point
of view, it remains unclear why transit times differ (Figure 4 and 5) and whether NPP or C_{veg} dominates the biases. Based on
Figure 4 and 5, biases in biomass C stocks likely dominate the error in turnover times. We used CARDAMOM to calculate

390 the relative contribution of productivity and biomass to the transit times bias by applying a simple attribution analysis (Figure
6). The largest bias to transit times are originated by modest understanding of the biomass component. Therefore, this study
agrees with previous studies (Friend et al., 2014; Nishina et al., 2014; Thurner et al., 2017) highlighting the deficient
representation of turnover dynamics, but we further suggest that GVM and ESM modellers need to focus on the vegetation C
stocks dynamics calculations to improve inner dynamics.

395

Earth System
Dynamics
Discussions

4.3 Outlook

CARDAMOM estimates for pan-Arctic C cycling are in good agreement with observations and data constraints; however, we have not included important components controlling ecosystem processes that could potentially improve our understanding on C feedbacks, and with emphasis for high latitude ecosystems. For example, thaw and release of permafrost

400   C is not represented in CARDAMOM, but the influence on vegetation dynamics, permafrost degradation and soil respiration is critical in high latitudes (Koven et al., 2015b; Parazoo et al., 2018). Also, Koven et al. (2017) shown that soil thermal regimes are key to getting the long-term vulnerability of soil C right. Moreover, we have not characterized snow dynamics and the insulating effect of snow affecting respiratory losses across wintertime periods either (Essery, 2015). Further, methane emissions, another important contributor to total C budget (Mastepanov et al., 2008; Mastepanov et al., 2012; Zona et al.,

405   2016), was neglected from this modelling exercise, although it is not easy to model due to its complex transport mechanisms (Kaiser et al., 2017; Walter et al., 2001).

In order to decrease uncertainties around the balance of photosynthetic inputs and respiratory outputs, future explorations on SOC decomposition by microbial activity (Xenakis and Williams, 2014), nutrient interaction with carbon (Thomas and Williams, 2014), plant traits relationships across pan-arctic regions (Reichstein et al., 2014; Sloan et al., 2013),

410   the mechanisims driving carbon use efficiency (Bradford and Crowther, 2013; Street et al., 2013) and the drivers of gross flux coupling (López-Blanco et al., 2017), or the effect of fine-scale disturbances such as moth outbreaks (Heliasz et al., 2011; López-Blanco et al., 2017; Lund et al., 2017) should be addressed at the pan-Arctic scale. From a modelling perspective, we consider that more field observations are crucial, specifically on plant and soil decomposition (C stocks turnover rates)(He et al., 2016) and respiratory processes (partitioning of R_{eco} into R_a and R_h) (Hobbie et al., 2000; McGuire et al., 2000), not only

415   across the growing season, but also during wintertime (Commane et al., 2017; Zona et al., 2016). An improved data-model integration will move towards enhanced model robustness and the decrease of its uncertainties. Field and model researchers should work on data model integration, not just driven based on data availability.

5 Conclusions

The Arctic is experiencing rapid environmental changes, which are expected to significantly influence the global C

420   cycle. Using a data-assimilation framework we have evaluated the current state of key C flux, stocks and transit time variables for the pan-Arctic region. We successfully assimilated SOC and biomass, and showed that biomass constraints have a greater importance for contemporary C dynamics (such as C stocks and transit times) than soil C data, which suggest that short term processes are more important than the long term for monthly to annual C dynamics. However, on the longer term, the much greater stock of C in slower stocks means that e.g. the permafrost carbon-climate feedback, will likely have important

425   consequences for arctic and global carbon cycling (Koven et al., 2015b). We found that our pan-Arctic estimates of C cycling retrievals are consistent with previous studies. Comparisons with global and local scale datasets demonstrate the advantageus capabilities of CARDAMOM assessing the C cycling in the Arctic domain. Moreover, CARDAMOM is a more data-constrained and data-integrated approach than any GVMs available, thus data-assimilation systems are good candidates to benchmark a forward model's performance, and pinpoint issues that need attention. We found better agreement for NPP

430   estimates than for biomass, which is the main contributor to transit time bias. Improved mapping of vegetation C stocks and change over time is required for better analytical constraint. Moreover, future work is required with modelling of soil thermal regimes, permafrost and snow dynamics to improve accuracy and decrease uncertainties. This work establishes the baseline for more process-based ecological analyses using the CARDAMOM data-assimilation system as a promising technique to constrain the pan-Arctic C cycle.

Earth System
Dynamics
Discussions

Data availability

CARDAMOM output used in this study is available from Exbrayat and Williams (2018) from the University of Edinburgh's DataShare service at http://dx.doi.org/10.7488/ds/2334.

Acknowledgements

References

Abbott, B. W., Jones, J. B., Schuur, E. A. G., Chapin, F. S., Bowden, W. B., Bret-Harte, M. S., Epstein, H. E., Flannigan, M. D., Harms, T. K., Hollingsworth, T. N., Mack, M. C., McGuire, A. D., Natali, S. M., Rocha, A. V., Tank, S. E., Turetsky, M. R., Vonk, J. E., Wickland, K. P., Aiken, G. R., Alexander, H. D., Amon, R. M. W., Benscoter, B. W., Bergeron, Y., Bishop, K., Blarquez, O., Bond-Lamberty, B., Breen, A. L., Buffam, I., Cai, Y., Carcaillet, C., Carey, S. K., Chen, J. M., Chen, H. Y. H., Christensen, T. R., Cooper, L. W., Cornelissen, J. H. C., De Groot, W. J., Deluca, T. H., Dorrepaal, E., Fetcher, N., Finlay, J. C., Forbes, B. C., French, N. H. F., Gauthier, S., Girardin, M. P., Goetz, S. J., Goldammer, J. G., Gough, L., Grogan, P., Guo, L., Higuera, P. E., Hinzman, L., Hu, F. S., Hugelius, G., Jafarov, E. E., Jandt, R., Johnstone, J. F., Karlsson, J., Kasischke, E. S., Kattner, G., Kelly, R., Keuper, F., Kling, G. W., Kortelainen, P., Kouki, J., Kuhry, P., Laudon, H., Laurion, I., MacDonald, R. W., Mann, P. J., Martikainen, P. J., McClelland, J. W., Molau, U., Oberbauer, S. F., Olefeldt, D., Paré, D., Parisien, M. A., Payette, S., Peng, C., Pokrovsky, O. S., Rastetter, E. B., Raymond, P. A., Raynolds, M. K., Rein, G., Reynolds, J. F., Robards, M., Rogers, B. M., Schdel, C., Schaefer, K., Schmidt, I. K., Shvidenko, A., Sky, J., Spencer, R. G. M., Starr, G., Striegl, R. G., Teisserenc, R., Tranvik, L. J., Virtanen, T., Welker, J. M., and Zimov, S.: Biomass offsets little or none of permafrost carbon release from soils, streams, and wildfire: an expert assessment, Environmental Research Letters, 11, 034014, 2016.

Ahlström, A., Schurgers, G., Arneth, A., and Smith, B.: Robustness and uncertainty in terrestrial ecosystem carbon response to CMIP5 climate change projections, Environmental Research Letters, 7, 044008, 2012.

AMAP: Snow, water, ice and permafrost in the Arctic (SWIPA) 2017, Oslo, Norway, xiv + 269 pp, 2017.

Anav, A., Murray-Tortarolo, G., Friedlingstein, P., Sitch, S., Piao, S., and Zhu, Z.: Evaluation of Land Surface Models in Reproducing Satellite Derived Leaf Area Index over the High-Latitude Northern Hemisphere. Part II: Earth System Models, Remote Sensing, 5, 3637, 2013.

Arora, V. K., Boer, G. J., Friedlingstein, P., Eby, M., Jones, C. D., Christian, J. R., Bonan, G., Bopp, L., Brovkin, V., Cadule, P., Hajima, T., Ilyina, T., Lindsay, K., Tjiputra, J. F., and Wu, T.: Carbon–Concentration and Carbon–Climate Feedbacks in CMIP5 Earth System Models, Journal of Climate, 26, 5289-5314, 10.1175/jcli-d-12-00494.1, 2013.

Baldocchi, D. D.: Assessing the eddy covariance technique for evaluating carbon dioxide exchange rates of ecosystems: past, present and future, Global Change Biology, 9, 479-492, 10.1046/j.1365-2486.2003.00629.x, 2003.

Belelli Marchesini, L., Papale, D., Reichstein, M., Vuichard, N., Tchebakova, N., and Valentini, R.: Carbon balance assessment of a natural steppe of southern Siberia by multiple constraint approach, Biogeosciences, 4, 581-595, 10.5194/bg-4-581-2007, 2007.

Bentsen, M., Bethke, I., Debernard, J. B., Iversen, T., Kirkevåg, A., Seland, Ã., Drange, H., Roelandt, C., Seierstad, I. A., Hoose, C., and Kristjánsson, J. E.: The Norwegian Earth System Model, NorESM1-M – Part 1: Description and basic evaluation of the physical climate, Geosci. Model Dev., 6, 687-720, 10.5194/gmd-6-687-2013, 2013.

Bloom, A. A., and Williams, M.: Constraining ecosystem carbon dynamics in a data-limited world: integrating ecological "common sense" in a model–data fusion framework, Biogeosciences, 12, 1299-1315, 10.5194/bg-12-1299-2015, 2015.

Bloom, A. A., Exbrayat, J.-F., van der Velde, I. R., Feng, L., and Williams, M.: The decadal state of the terrestrial carbon cycle: Global retrievals of terrestrial carbon allocation, pools, and residence times, Proceedings of the National Academy of Sciences, 113, 1285-1290, 10.1073/pnas.1515160113, 2016.

Bond-Lamberty, B., Wang, C., and Gower, S. T.: Net primary production and net ecosystem production of a boreal black spruce wildfire chronosequence, Global Change Biology, 10, 473-487, doi:10.1111/j.1529-8817.2003.0742.x, 2004.

Bontemps, S., Defourny, P., Bogaert, E., Arino, O., Kalogirou, V., and Perez, J.: GLOBCOVER 2009 - Products description and validation report, 2011.

Bradford, M. A., and Crowther, T. W.: Carbon use efficiency and storage in terrestrial ecosystems, New Phytologist, 199, 7-9, 10.1111/nph.12334, 2013.

Brown, J., Ferrians Jr, O. J., Heginbottom, J. A., and Melnikov, E. S.: Circum-Arctic map of permafrost and ground-ice conditions, Report 45, 1997.

Canadell, J. G., Le Quéré, C., Raupach, M. R., Field, C. B., Buitenhuis, E. T., Ciais, P., Conway, T. J., Gillett, N. P., Houghton, R. A., and Marland, G.: Contributions to accelerating atmospheric CO_2 growth from economic activity, carbon intensity, and efficiency of natural sinks, Proceedings of the National Academy of Sciences, 104, 18866-18870, 10.1073/pnas.0702737104, 2007.

Carvalhais, N., Forkel, M., Khomik, M., Bellarby, J., Jung, M., Migliavacca, M., u, M., Saatchi, S., Santoro, M., Thurner, M., Weber, U., Ahrens, B., Beer, C., Cescatti, A., Randerson, J. T., and Reichstein, M.: Global covariation of carbon turnover times with climate in terrestrial ecosystems, Nature, 514, 213-217, 10.1038/nature13731, 2014.

Ceballos-Núñez, V., Richardson, A. D., and Sierra, C. A.: Ages and transit times as important diagnostics of model performance for predicting carbon dynamics in terrestrial vegetation models, Biogeosciences Discuss., 2017, 1-27, 10.5194/bg-2017-308, 2017.

Clark, D. B., Mercado, L. M., Sitch, S., Jones, C. D., Gedney, N., Best, M. J., Pryor, M., Rooney, G. G., Essery, R. L. H., Blyth, E., Boucher, O., Harding, R. J., Huntingford, C., and Cox, P. M.: The Joint UK Land Environment Simulator (JULES), model description – Part 2: Carbon fluxes and vegetation dynamics, Geosci. Model Dev., 4, 701-722, 10.5194/gmd-4-701-2011, 2011.

Collins, W. J., Bellouin, N., Doutriaux-Boucher, M., Gedney, N., Halloran, P., Hinton, T., Hughes, J., Jones, C. D., Joshi, M., Liddicoat, S., Martin, G., O'Connor, F., Rae, J., Senior, C., Sitch, S., Totterdell, I., Wiltshire, A., and Woodward, S.: Development and evaluation of an Earth-System model – HadGEM2, Geosci. Model Dev., 4, 1051-1075, 10.5194/gmd-4-1051-2011, 2011.

Commane, R., Lindaas, J., Benmergui, J., Luus, K. A., Chang, R. Y.-W., Daube, B. C., Euskirchen, E. S., Henderson, J. M., Karion, A., Miller, J. B., Miller, S. M., Parazoo, N. C., Randerson, J. T., Sweeney, C., Tans, P., Thoning, K., Veraverbeke, S., Miller, C. E., and Wofsy, S. C.: Carbon dioxide sources from Alaska driven by increasing early winter respiration from Arctic tundra, Proceedings of the National Academy of Sciences, 114, 5361-5366, 10.1073/pnas.1618567114, 2017.

Cox, P. M.: Description of the "TRIFFID" Dynamic Global Vegetation Model. Hadley Centre technical note 24, Met Office, UK, 2001.

Dee, D. P., Uppala, S. M., Simmons, A. J., Berrisford, P., Poli, P., Kobayashi, S., Andrae, U., Balmaseda, M. A., Balsamo, G., Bauer, P., Bechtold, P., Beljaars, A. C. M., van de Berg, L., Bidlot, J., Bormann, N., Delsol, C., Dragani, R., Fuentes, M., Geer, A. J., Haimberger, L., Healy, S. B., Hersbach, H., Hólm, E. V., Isaksen, L., Kållberg, P., Köhler, M., Matricardi, M., McNally, A. P., Monge-Sanz, B. M., Morcrette, J. J., Park, B. K., Peubey, C., de Rosnay, P., Tavolato, C., Thépaut, J. N., and Vitart, F.: The ERA-Interim reanalysis: configuration and performance of the data assimilation system, Quarterly Journal of the Royal Meteorological Society, 137, 553-597, 10.1002/qj.828, 2011.

530 Dufresne, J.-L., Foujols, M.-A., Denvil, S., Caubel, A., Marti, O., Aumont, O., Balkanski, Y., Bekki, S., Bellenger, H., Benshila, R., Bony, S., Bopp, L., Braconnot, P., Brockmann, P., Cadule, P., Cheruy, F., Codron, F., Cozic, A., Cugnet, D., de Noblet, N., Duvel, J.-P., Ethé, C., Fairhead, L., Fichefet, T., Flavoni, S., Friedlingstein, P., Grandpeix, J.-Y., Guez, L., Guilyardi, E., Hauglustaine, D., Hourdin, F., Idelkadi, A., Ghattas, J., Joussaume, S., Kageyama, M., Krinner, G., Labetoulle, S., Lahellec, A., Lefebvre, M.-P., Lefevre, F., Levy, C., Li, Z. X., Lloyd, J., Lott, F., Madec, G., Mancip, M., Marchand, M., Masson, S., Meurdesoif, Y., Mignot, J., Musat, I., Parouty, S., Polcher, J., Rio, C., Schulz, M., Swingedouw, D., Szopa, S., Talandier, C., Terray, P., Viovy, N., and Vuichard, N.: Climate change projections using the IPSL-CM5 Earth System Model: from CMIP3 to CMIP5, Climate Dynamics, 40, 2123-2165, 10.1007/s00382-012-1636-1, 2013.

535 Dunne, J. P., John, J. G., Adcroft, A. J., Griffies, S. M., Hallberg, R. W., Shevliakova, E., Stouffer, R. J., Cooke, W., Dunne, K. A., Harrison, M. J., Krasting, J. P., Malyshev, S. L., Milly, P. C. D., Phillipps, P. J., Sentman, L. T., Samuels, B. L., Spelman, M. J., Winton, M., Wittenberg, A. T., and Zadeh, N.: GFDL's ESM2 Global Coupled Climate–Carbon Earth System Models. Part I: Physical Formulation and Baseline Simulation Characteristics, Journal of Climate, 25, 6646-6665, 10.1175/jcli-d-11-00560.1, 2012.

540 Essery, R.: A factorial snowpack model (FSM 1.0), Geosci. Model Dev., 8, 3867-3876, 10.5194/gmd-8-3867-2015, 2015.

Exbrayat, J. F., Bloom, A. A., Falloon, P., Ito, A., Smallman, T. L., and Williams, M.: Reliability ensemble averaging of 21st century projections of terrestrial net primary productivity reduces global and regional uncertainties, Earth Syst. Dynam., 9, 153-165, 10.5194/esd-9-153-2018, 2018.

Exbrayat, J. F., and Williams, M.: CARDAMOM panarctic retrievals 2000-2015. 2000-2015 [Dataset], National Centre for
545 Earth Observation and School of GeoSciences. University of Edinburgh, http://dx.doi.org/10.7488/ds/2334, 2018.

FAO/IIASA/ISRIC/ISSCAS/JRC: Harmonized World Soil Database (version 1.21). FAO, Rome, Italy and IIASA, Laxenburg, Austria, 2012.

Fisher, J. B., Sikka, M., Oechel, W. C., Huntzinger, D. N., Melton, J. R., Koven, C. D., Ahlström, A., Arain, M. A., Baker, I., Chen, J. M., Ciais, P., Davidson, C., Dietze, M., El-Masri, B., Hayes, D., Huntingford, C., Jain, A. K., Levy, P. E., Lomas, M.
550 R., Poulter, B., Price, D., Sahoo, A. K., Schaefer, K., Tian, H., Tomelleri, E., Verbeeck, H., Viovy, N., Wania, R., Zeng, N., and Miller, C. E.: Carbon cycle uncertainty in the Alaskan Arctic, Biogeosciences, 11, 4271-4288, 10.5194/bg-11-4271-2014, 2014.

Friedlingstein, P., Meinshausen, M., Arora, V. K., Jones, C. D., Anav, A., Liddicoat, S. K., and Knutti, R.: Uncertainties in CMIP5 Climate Projections due to Carbon Cycle Feedbacks, Journal of Climate, 27, 511-526, 10.1175/jcli-d-12-00579.1,
555 2014.

Friend, A. D., and White, A.: Evaluation and analysis of a dynamic terrestrial ecosystem model under preindustrial conditions at the global scale, Global Biogeochemical Cycles, 14, 1173-1190, doi:10.1029/1999GB900085, 2000.

Friend, A. D., Lucht, W., Rademacher, T. T., Keribin, R., Betts, R., Cadule, P., Ciais, P., Clark, D. B., Dankers, R., Falloon, P. D., Ito, A., Kahana, R., Kleidon, A., Lomas, M. R., Nishina, K., Ostberg, S., Pavlick, R., Peylin, P., Schaphoff, S., Vuichard,
560 N., Warszawski, L., Wiltshire, A., and Woodward, F. I.: Carbon residence time dominates uncertainty in terrestrial vegetation responses to future climate and atmospheric CO2, Proceedings of the National Academy of Sciences, 111, 3280-3285, 10.1073/pnas.1222477110, 2014.

Goulden, M. L., Munger, J. W., Fan, S.-M., Daube, B. C., and Wofsy, S. C.: Exchange of Carbon Dioxide by a Deciduous Forest: Response to Interannual Climate Variability, Science, 271, 1576-1578, 10.1126/science.271.5255.1576, 1996.

565 Grøndahl, L., Friborg, T., Christensen, T. R., Ekberg, A., Elberling, B., Illeris, L., Nordstrøm, C., Rennermalm, Å., Sigsgaard, C., and Søgaard, H.: Spatial and Inter-Annual Variability of Trace Gas Fluxes in a Heterogeneous High-Arctic Landscape, in: Advances in Ecological Research, edited by: Hans Meltofte, T. R. C. B. E. M. C. F., and Morten, R., Academic Press, 473-498, 2008.

Hashimoto, S., Carvalhais, N., Ito, A., Migliavacca, M., Nishina, K., and Reichstein, M.: Global spatiotemporal distribution
570 of soil respiration modeled using a global database, Biogeosciences, 12, 4121-4132, 10.5194/bg-12-4121-2015, 2015.

He, Y., Trumbore, S. E., Torn, M. S., Harden, J. W., Vaughn, L. J. S., Allison, S. D., and Randerson, J. T.: Radiocarbon constraints imply reduced carbon uptake by soils during the 21st century, Science, 353, 1419-1424, 10.1126/science.aad4273, 2016.

Heliasz, M., Johansson, T., Lindroth, A., Mölder, M., Mastepanov, M., Friborg, T., Callaghan, T. V., and Christensen, T. R.:
575 Quantification of C uptake in subarctic birch forest after setback by an extreme insect outbreak, Geophysical Research Letters, 38, n/a-n/a, 10.1029/2010GL044733, 2011.

Earth System
Dynamics
Discussions

Hempel, S., Frieler, K., Warszawski, L., Schewe, J., and Piontek, F.: A trend-preserving bias correction – the ISI-MIP approach, Earth Syst. Dynam., 4, 219-236, 10.5194/esd-4-219-2013, 2013.

580 Hobbie, S. E., Schimel, J. P., Trumbore, S. E., and Randerson, J. R.: Controls over carbon storage and turnover in high-latitude soils, Global Change Biology, 6, 196-210, 10.1046/j.1365-2486.2000.06021.x, 2000.

Hugelius, G., Bockheim, J. G., Camill, P., Elberling, B., Grosse, G., Harden, J. W., Johnson, K., Jorgenson, T., Koven, C. D., Kuhry, P., Michaelson, G., Mishra, U., Palmtag, J., Ping, C. L., O'Donnell, J., Schirrmeister, L., Schuur, E. A. G., Sheng, Y., Smith, L. C., Strauss, J., and Yu, Z.: A new data set for estimating organic carbon storage to 3 m depth in soils of the northern circumpolar permafrost region, Earth Syst. Sci. Data, 5, 393-402, 10.5194/essd-5-393-2013, 2013a.

585 Hugelius, G., Tarnocai, C., Broll, G., Canadell, J. G., Kuhry, P., and Swanson, D. K.: The Northern Circumpolar Soil Carbon Database: spatially distributed datasets of soil coverage and soil carbon storage in the northern permafrost regions, Earth Syst. Sci. Data, 5, 3-13, 10.5194/essd-5-3-2013, 2013b.

Hugelius, G., Strauss, J., Zubrzycki, S., Harden, J. W., Schuur, E. A. G., Ping, C. L., Schirrmeister, L., Grosse, G., Michaelson, G. J., Koven, C. D., O'Donnell, J. A., Elberling, B., Mishra, U., Camill, P., Yu, Z., Palmtag, J., and Kuhry, P.: Improved 590 estimates show large circumpolar stocks of permafrost carbon while quantifying substantial uncertainty ranges and identifying remaining data gaps, Biogeosciences Discuss., 11, 4771-4822, 10.5194/bgd-11-4771-2014, 2014.

Ikawa, H., Nakai, T., Busey, R. C., Kim, Y., Kobayashi, H., Nagai, S., Ueyama, M., Saito, K., Nagano, H., Suzuki, R., and Hinzman, L.: Understory CO2, sensible heat, and latent heat fluxes in a black spruce forest in interior Alaska, Agricultural and Forest Meteorology, 214-215, 80-90, https://doi.org/10.1016/j.agrformet.2015.08.247, 2015.

595 Ito, A., and Inatomi, M.: Water-Use Efficiency of the Terrestrial Biosphere: A Model Analysis Focusing on Interactions between the Global Carbon and Water Cycles, Journal of Hydrometeorology, 13, 681-694, 10.1175/jhm-d-10-05034.1, 2012.

Jackson, R. B., Lajtha, K., Crow, S. E., Hugelius, G., Kramer, M. G., and Piñeiro, G.: The Ecology of Soil Carbon: Pools, Vulnerabilities, and Biotic and Abiotic Controls, Annual Review of Ecology, Evolution, and Systematics, 48, 419-445, 10.1146/annurev-ecolsys-112414-054234, 2017.

600 Jung, M., Reichstein, M., Margolis, H. A., Cescatti, A., Richardson, A. D., Arain, M. A., Arneth, A., Bernhofer, C., Bonal, D., Chen, J., Gianelle, D., Gobron, N., Kiely, G., Kutsch, W., Lasslop, G., Law, B. E., Lindroth, A., Merbold, L., Montagnani, L., Moors, E. J., Papale, D., Sottocornola, M., Vaccari, F., and Williams, C.: Global patterns of land-atmosphere fluxes of carbon dioxide, latent heat, and sensible heat derived from eddy covariance, satellite, and meteorological observations, Journal of Geophysical Research: Biogeosciences, 116, doi:10.1029/2010JG001566, 2011.

605 Jung, M., Reichstein, M., Schwalm, C. R., Huntingford, C., Sitch, S., Ahlström, A., Arneth, A., Camps-Valls, G., Ciais, P., Friedlingstein, P., Gans, F., Ichii, K., Jain, A. K., Kato, E., Papale, D., Poulter, B., Raduly, B., Rödenbeck, C., Tramontana, G., Viovy, N., Wang, Y.-P., Weber, U., Zaehle, S., and Zeng, N.: Compensatory water effects link yearly global land CO2 sink changes to temperature, Nature, 541, 516, 10.1038/nature20780, 2017.

Kaiser, S., Göckede, M., Castro-Morales, K., Knoblauch, C., Ekici, A., Kleinen, T., Zubrzycki, S., Sachs, T., Wille, C., and 610 Beer, C.: Process-based modelling of the methane balance in periglacial landscapes (JSBACH-methane), Geosci. Model Dev., 10, 333-358, 10.5194/gmd-10-333-2017, 2017.

Kimball, J. S., Jones, L. A., Zhang, K., Heinsch, F. A., McDonald, K. C., and Oechel, W.: A Satellite Approach to Estimate Land CO2 Exchange for Boreal and Arctic Biomes Using MODIS and AMSR-E, IEEE Transactions on Geoscience and Remote Sensing, 47, 569-587, 10.1109/TGRS.2008.2003248, 2009.

615 Koven, C. D., Ringeval, B., Friedlingstein, P., Ciais, P., Cadule, P., Khvorostyanov, D., Krinner, G., and Tarnocai, C.: Permafrost carbon-climate feedbacks accelerate global warming, Proceedings of the National Academy of Sciences, 108, 14769-14774, 10.1073/pnas.1103910108, 2011.

Koven, C. D., Schuur, E. A. G., Schädel, C., Bohn, T. J., Burke, E. J., Chen, G., Chen, X., Ciais, P., Grosse, G., Harden, J. W., Hayes, D. J., Hugelius, G., Jafarov, E. E., Krinner, G., Kuhry, P., Lawrence, D. M., MacDougall, A. H., Marchenko, S. S., 620 McGuire, A. D., Natali, S. M., Nicolsky, D. J., Olefeldt, D., Peng, S., Romanovsky, V. E., Schaefer, K. M., Strauss, J., Treat, C. C., and Turetsky, M.: A simplified, data-constrained approach to estimate the permafrost carbon–climate feedback, Philosophical Transactions of the Royal Society A: Mathematical, Physical and Engineering Sciences, 373, 10.1098/rsta.2014.0423, 2015a.

Koven, C. D., Schuur, E. A. G., Schädel, C., Bohn, T. J., Burke, E. J., Chen, G., Chen, X., Ciais, P., Grosse, G., Harden, J. W., 625 Hayes, D. J., Hugelius, G., Jafarov, E. E., Krinner, G., Kuhry, P., Lawrence, D. M., MacDougall, A. H., Marchenko, S. S., McGuire, A. D., Natali, S. M., Nicolsky, D. J., Olefeldt, D., Peng, S., Romanovsky, V. E., Schaefer, K. M., Strauss, J., Treat,

Earth System
Dynamics

Discussions

C. C., and Turetsky, M.: A simplified, data-constrained approach to estimate the permafrost carbon–climate feedback, Philosophical Transactions of the Royal Society A: Mathematical, Physical and Engineering Sciences, 373, 10.1098/rsta.2014.0423, 2015b.

630 Koven, C. D., Hugelius, G., Lawrence, D. M., and Wieder, W. R.: Higher climatological temperature sensitivity of soil carbon in cold than warm climates, Nature Climate Change, 7, 817, 10.1038/nclimate3421, 2017.

Kutzbach, L., Wille, C., and Pfeiffer, E.-M.: The exchange of carbon dioxide between wet arctic tundra and the atmosphere at the Lena River Delta, Northern Siberia, Biogeosciences, 4, 869-890, 10.5194/bg-4-869-2007, 2007.

Lafleur, P. M., Humphreys, E. R., St. Louis, V. L., Myklebust, M. C., Papakyriakou, T., Poissant, L., Barker, J. D., Pilote, M.,
635 and Swystun, K. A.: Variation in Peak Growing Season Net Ecosystem Production Across the Canadian Arctic, Environmental Science & Technology, 46, 7971-7977, 10.1021/es300500m, 2012.

Lasslop, G., Reichstein, M., Papale, D., Richardson, A. D., Arneth, A., Barr, A., Stoy, P., and Wohlfahrt, G.: Separation of net ecosystem exchange into assimilation and respiration using a light response curve approach: critical issues and global evaluation, Global Change Biology, 16, 187-208, 10.1111/j.1365-2486.2009.02041.x, 2010.

640 Lawrence, D. M., Oleson, K. W., Flanner, M. G., Thornton, P. E., Swenson, S. C., Lawrence, P. J., Zeng, X., Yang, Z. L., Levis, S., Sakaguchi, K., Bonan, G. B., and Slater, A. G.: Parameterization improvements and functional and structural advances in Version 4 of the Community Land Model, Journal of Advances in Modeling Earth Systems, 3, doi:10.1029/2011MS00045, 2011.

Le Quéré, C., Andrew, R. M., Friedlingstein, P., Sitch, S., Pongratz, J., Manning, A. C., Korsbakken, J. I., Peters, G. P.,
645 Canadell, J. G., Jackson, R. B., Boden, T. A., Tans, P. P., Andrews, O. D., Arora, V. K., Bakker, D. C. E., Barbero, L., Becker, M., Betts, R. A., Bopp, L., Chevallier, F., Chini, L. P., Ciais, P., Cosca, C. E., Cross, J., Currie, K., Gasser, T., Harris, I., Hauck, J., Haverd, V., Houghton, R. A., Hunt, C. W., Hurtt, G., Ilyina, T., Jain, A. K., Kato, E., Kautz, M., Keeling, R. F., Klein Goldewijk, K., Körtzinger, A., Landschützer, P., Lefèvre, N., Lenton, A., Lienert, S., Lima, I., Lombardozzi, D., Metzl, N., Millero, F., Monteiro, P. M. S., Munro, D. R., Nabel, J. E. M. S., Nakaoka, S.-I., Nojiri, Y., Padin, X. A., Peregon, A.,
650 Pfeil, B., Pierrot, D., Poulter, B., Rehder, G., Reimer, J., Rödenbeck, C., Schwinger, J., Séférian, R., Skjelvan, I., Stocker, B. D., Tian, H., Tilbrook, B., Tubiello, F. N., van der Laan-Luijkx, I. T., van der Werf, G. R., van Heuven, S., Viovy, N., Vuichard, N., Walker, A. P., Watson, A. J., Wiltshire, A. J., Zaehle, S., and Zhu, D.: Global Carbon Budget 2017, Earth Syst. Sci. Data, 10, 405-448, 10.5194/essd-10-405-2018, 2018.

Levy, P. E., Friend, A. D., White, A., and Cannell, M. G. R.: 'The Influence of Land Use Change On Global-Scale Fluxes of
655 Carbon from Terrestrial Ecosystems', Climatic Change, 67, 185-209, 10.1007/s10584-004-2849-z, 2004.

López-Blanco, E., Lund, M., Williams, M., Tamstorf, M. P., Westergaard-Nielsen, A., Exbrayat, J. F., Hansen, B. U., and Christensen, T. R.: Exchange of CO_2 in Arctic tundra: impacts of meteorological variations and biological disturbance, Biogeosciences, 14, 4467-4483, 10.5194/bg-14-4467-2017, 2017.

Lucht, W., Prentice, I. C., Myneni, R. B., Sitch, S., Friedlingstein, P., Cramer, W., Bousquet, P., Buermann, W., and Smith,
660 B.: Climatic Control of the High-Latitude Vegetation Greening Trend and Pinatubo Effect, Science, 296, 1687-1689, 10.1126/science.1071828, 2002.

Lund, M., Falk, J. M., Friborg, T., Mbufong, H. N., Sigsgaard, C., Soegaard, H., and Tamstorf, M. P.: Trends in CO_2 exchange in a high Arctic tundra heath, 2000-2010, Journal of Geophysical Research: Biogeosciences, 117, 2012.

Lund, M., Raundrup, K., Westergaard-Nielsen, A., López-Blanco, E., Nymand, J., and Aastrup, P.: Larval outbreaks in West
665 Greenland: Instant and subsequent effects on tundra ecosystem productivity and CO(2) exchange, AMBIO, 46, 26-38, 10.1007/s13280-016-0863-9, 2017.

Mastepanov, M., Sigsgaard, C., Dlugokencky, E. J., Houweling, S., Strom, L., Tamstorf, M. P., and Christensen, T. R.: Large tundra methane burst during onset of freezing, Nature, 456, 628-630, 10.1038/nature07464, 2008.

Mastepanov, M., Sigsgaard, C., Tagesson, T., Ström, L., Tamstorf, M. P., Lund, M., and Christensen, T. R.: Revisiting factors
670 controlling methane emissions from high-arctic tundra, Biogeosciences Discuss., 9, 15853-15900, 10.5194/bgd-9-15853-2012, 2012.

McGuire, A. D., Melillo, J. M., Randerson, J. T., Parton, W. J., Heimann, M., Meier, R. A., Clein, J. S., Kicklighter, D. W., and Sauf, W.: Modeling the effects of snowpack on heterotrophic respiration across northern temperate and high latitude regions: Comparison with measurements of atmospheric carbon dioxide in high latitudes, Biogeochemistry, 48, 91-114,
675 10.1023/a:1006286804351, 2000.

McGuire, A. D., Anderson, L. G., Christensen, T. R., Dallimore, S., Guo, L., Hayes, D. J., Heimann, M., Lorenson, T. D., Macdonald, R. W., and Roulet, N. T.: Sensitivity of the carbon cycle in the Arctic to climate change, Ecological Monographs, 79, 523-555, 10.1890/08-2025.1, 2009.

680 McGuire, A. D., Hayes, D., Kicklighter, D. W., Manizza, M., Zhuang, Q., Chen, M., Follows, M. J., Gurney, K. R., Mcclelland, J. W., Melillo, J. M., Peterson, B. J., and Prinn, R. G.: An analysis of the carbon balance of the Arctic Basin from 1997 to 2006, Tellus B, 62, 455-474, doi:10.1111/j.1600-0889.2010.00497.x, 2010.

McGuire, A. D., Christensen, T. R., Hayes, D., Heroult, A., Euskirchen, E., Kimball, J. S., Koven, C., Lafleur, P., Miller, P. A., Oechel, W., Peylin, P., Williams, M., and Yi, Y.: An assessment of the carbon balance of Arctic tundra: comparisons among observations, process models, and atmospheric inversions, Biogeosciences, 9, 3185-3204, 10.5194/bg-9-3185-2012, 685 2012.

Murray-Tortarolo, G., Anav, A., Friedlingstein, P., Sitch, S., Piao, S., Zhu, Z., Poulter, B., Zaehle, S., Ahlström, A., Lomas, M., Levis, S., Viovy, N., and Zeng, N.: Evaluation of Land Surface Models in Reproducing Satellite-Derived LAI over the High-Latitude Northern Hemisphere. Part I: Uncoupled DGVMs, Remote Sensing, 5, 4819, 2013.

Myers-Smith, I. H., Elmendorf, S. C., Beck, P. S. A., Wilmking, M., Hallinger, M., Blok, D., Tape, K. D., Rayback, S. A., 690 Macias-Fauria, M., Forbes, B. C., Speed, J. D. M., Boulanger-Lapointe, N., Rixen, C., Lévesque, E., Schmidt, N. M., Baittinger, C., Trant, A. J., Hermanutz, L., Collier, L. S., Dawes, M. A., Lantz, T. C., Weijers, S., Jørgensen, R. H., Buchwal, A., Buras, A., Naito, A. T., Ravolainen, V., Schaepman-Strub, G., Wheeler, J. A., Wipf, S., Guay, K. C., Hik, D. S., and Vellend, M.: Climate sensitivity of shrub growth across the tundra biome, Nature Climate Change, 5, 887, 10.1038/nclimate2697, 2015.

695 Myneni, R. B., Keeling, C. D., Tucker, C. J., Asrar, G., and Nemani, R. R.: Increased plant growth in the northern high latitudes from 1981 to 1991, Nature, 386, 698, 10.1038/386698a0, 1997.

Myneni, R. B., Hoffman, S., Knyazikhin, Y., Privette, J. L., Glassy, J., Tian, Y., Wang, Y., Song, X., Zhang, Y., Smith, G. R., Lotsch, A., Friedl, M., Morisette, J. T., Votava, P., Nemani, R. R., and Running, S. W.: Global products of vegetation leaf area and fraction absorbed PAR from year one of MODIS data, Remote Sensing of Environment, 83, 214-231, 700 https://doi.org/10.1016/S0034-4257(02)00074-3, 2002.

Nishina, K., Ito, A., Beerling, D. J., Cadule, P., Ciais, P., Clark, D. B., Falloon, P., Friend, A. D., Kahana, R., Kato, E., Keribin, R., Lucht, W., Lomas, M., Rademacher, T. T., Pavlick, R., Schaphoff, S., Vuichard, N., Warszawaski, L., and Yokohata, T.: Quantifying uncertainties in soil carbon responses to changes in global mean temperature and precipitation, Earth Syst. Dynam., 5, 197-209, 10.5194/esd-5-197-2014, 2014.

705 Nishina, K., Ito, A., Falloon, P., Friend, A. D., Beerling, D. J., Ciais, P., Clark, D. B., Kahana, R., Kato, E., Lucht, W., Lomas, M., Pavlick, R., Schaphoff, S., Warszawaski, L., and Yokohata, T.: Decomposing uncertainties in the future terrestrial carbon budget associated with emission scenarios, climate projections, and ecosystem simulations using the ISI-MIP results, Earth Syst. Dynam., 6, 435-445, 10.5194/esd-6-435-2015, 2015.

Papale, D., Reichstein, M., Aubinet, M., Canfora, E., Bernhofer, C., Kutsch, W., Longdoz, B., Rambal, S., Valentini, R., 710 Vesala, T., and Yakir, D.: Towards a standardized processing of Net Ecosystem Exchange measured with eddy covariance technique: algorithms and uncertainty estimation, Biogeosciences, 3, 571-583, 10.5194/bg-3-571-2006, 2006.

Parazoo, N. C., Koven, C. D., Lawrence, D. M., Romanovsky, V., and Miller, C. E.: Detecting the permafrost carbon feedback: talik formation and increased cold-season respiration as precursors to sink-to-source transitions, The Cryosphere, 12, 123-144, 10.5194/tc-12-123-2018, 2018.

715 Pavlick, R., Drewry, D. T., Bohn, K., Reu, B., and Kleidon, A.: The Jena Diversity-Dynamic Global Vegetation Model (JeDi-DGVM): a diverse approach to representing terrestrial biogeography and biogeochemistry based on plant functional trade-offs, Biogeosciences, 10, 4137-4177, 10.5194/bg-10-4137-2013, 2013.

Peñuelas, J., Rutishauser, T., and Filella, I.: Phenology Feedbacks on Climate Change, Science, 324, 887-888, 10.1126/science.1173004, 2009.

720 Reichstein, M., Bahn, M., Mahecha, M. D., Kattge, J., and Baldocchi, D. D.: Linking plant and ecosystem functional biogeography, Proceedings of the National Academy of Sciences, 111, 13697-13702, 10.1073/pnas.1216065111, 2014.

Running, S. W., Nemani, R. R., Heinsch, F. A., Zhao, M., Reeves, M., and Hashimoto, H.: A Continuous Satellite-Derived Measure of Global Terrestrial Primary Production, BioScience, 54, 547-560, 10.1641/0006-3568(2004)054[0547:ACSMOG]2.0.CO;2, 2004.

725   Sari, J., Tarmo, V., Vladimir, K., Tuomas, L., Maiju, L., Juha, M., Johanna, N., Aleksi, R., Juha-Pekka, T., and Mika, A.: Spatial variation and seasonal dynamics of leaf-area index in the arctic tundra-implications for linking ground observations and satellite images, Environmental Research Letters, 12, 095002, 2017.

Schuur, E. A. G., McGuire, A. D., Schadel, C., Grosse, G., Harden, J. W., Hayes, D. J., Hugelius, G., Koven, C. D., Kuhry, P., Lawrence, D. M., Natali, S. M., Olefeldt, D., Romanovsky, V. E., Schaefer, K., Turetsky, M. R., Treat, C. C., and Vonk, J. 730   E.: Climate change and the permafrost carbon feedback, Nature, 520, 171-179, 10.1038/nature14338, 2015.

Sierra, C. A., Müller, M., Metzler, H., Manzoni, S., and Trumbore, S. E.: The muddle of ages, turnover, transit, and residence times in the carbon cycle, Global Change Biology, 23, 1763-1773, 10.1111/gcb.13556, 2017.

Sitch, S., Smith, B., Prentice, I. C., Arneth, A., Bondeau, A., Cramer, W., Kaplan, J. O., Levis, S., Lucht, W., Sykes, M. T., Thonicke, K., and Venevsky, S.: Evaluation of ecosystem dynamics, plant geography and terrestrial carbon cycling in the LPJ 735   dynamic global vegetation model, Global Change Biology, 9, 161-185, doi:10.1046/j.1365-2486.2003.00569.x, 2003.

Slevin, D., Tett, S. F. B., Exbrayat, J.-F., Bloom, A. A., and Williams, M.: Global evaluation of gross primary productivity in the JULES land surface model v3.4.1, Geosci. Model Dev., 10, 2651-2670, 10.5194/gmd-10-2651-2017, 2017.

Sloan, V. L., Fletcher, B. J., Press, M. C., Williams, M., and Phoenix, G. K.: Leaf and fine root carbon stocks and turnover are coupled across Arctic ecosystems, Global Change Biology, 19, 3668-3676, 10.1111/gcb.12322, 2013.

740   Smallman, T. L., Exbrayat, J.-F., Mencuccini, M., Bloom, A. A., and Williams, M.: Assimilation of repeated woody biomass observations constrains decadal ecosystem carbon cycle uncertainty in aggrading forests, Journal of Geophysical Research: Biogeosciences, 122, 528-545, doi:10.1002/2016JG003520, 2017.

Smith, B., Prentice, I. C., and Sykes, M. T.: Representation of vegetation dynamics in the modelling of terrestrial ecosystems: comparing two contrasting approaches within European climate space, Global Ecology and Biogeography, 10, 621-637, 745   doi:10.1046/j.1466-822X.2001.t01-1-00256.x, 2001.

Street, L. E., Subke, J.-A., Sommerkorn, M., Sloan, V., Ducrotoy, H., Phoenix, G. K., and Williams, M.: The role of mosses in carbon uptake and partitioning in arctic vegetation, New Phytologist, 199, 163-175, 10.1111/nph.12285, 2013.

Tarnocai, C., Canadell, J. G., Schuur, E. A. G., Kuhry, P., Mazhitova, G., and Zimov, S.: Soil organic carbon pools in the northern circumpolar permafrost region, Global Biogeochemical Cycles, 23, GB2023, 10.1029/2008GB003327, 2009.

750   Taylor, K. E., Stouffer, R. J., and Meehl, G. A.: An Overview of CMIP5 and the Experiment Design, Bulletin of the American Meteorological Society, 93, 485-498, 10.1175/bams-d-11-00094.1, 2012.

Thomas, R. Q., and Williams, M.: A model using marginal efficiency of investment to analyze carbon and nitrogen interactions in terrestrial ecosystems (ACONITE Version 1), Geosci. Model Dev., 7, 2015-2037, 10.5194/gmd-7-2015-2014, 2014.

Thornton, P. E., Doney, S. C., Lindsay, K., Moore, J. K., Mahowald, N., Randerson, J. T., Fung, I., Lamarque, J. F., Feddema, 755   J. J., and Lee, Y. H.: Carbon-nitrogen interactions regulate climate-carbon cycle feedbacks: results from an atmosphere-ocean general circulation model, Biogeosciences, 6, 2099-2120, 10.5194/bg-6-2099-2009, 2009.

Thurner, M., Beer, C., Santoro, M., Carvalhais, N., Wutzler, T., Schepaschenko, D., Shvidenko, A., Kompter, E., Ahrens, B., Levick, S. R., and Schmullius, C.: Carbon stock and density of northern boreal and temperate forests, Global Ecology and Biogeography, 23, 297-310, doi:10.1111/geb.12125, 2014.

760   Thurner, M., Beer, C., Ciais, P., Friend, A. D., Ito, A., Kleidon, A., Lomas, M. R., Quegan, S., Rademacher, T. T., Schaphoff, S., Tum, M., Wiltshire, A., and Carvalhais, N.: Evaluation of climate-related carbon turnover processes in global vegetation models for boreal and temperate forests, Global Change Biology, 23, 3076-3091, 10.1111/gcb.13660, 2017.

Tramontana, G., Jung, M., Schwalm, C. R., Ichii, K., Camps-Valls, G., Ráduly, B., Reichstein, M., Arain, M. A., Cescatti, A., Kiely, G., Merbold, L., Serrano-Ortiz, P., Sickert, S., Wolf, S., and Papale, D.: Predicting carbon dioxide and energy fluxes 765   across global FLUXNET sites with
regression algorithms, Biogeosciences, 13, 4291-4313, 10.5194/bg-13-4291-2016, 2017.

Tum, M., Zeidler, J. N., Günther, K. P., and Esch, T.: Global NPP and straw bioenergy trends for 2000–2014, Biomass and Bioenergy, 90, 230-236, https://doi.org/10.1016/j.biombioe.2016.03.040, 2016.

van der Molen, M. K., van Huissteden, J., Parmentier, F. J. W., Petrescu, A. M. R., Dolman, A. J., Maximov, T. C., Kononov, 770   A. V., Karsanaev, S. V., and Suzdalov, D. A.: The growing season greenhouse gas balance of a continental tundra site in the Indigirka lowlands, NE Siberia, Biogeosciences, 4, 985-1003, 10.5194/bg-4-985-2007, 2007.

Walter, B. P., Heimann, M., and Matthews, E.: Modeling modern methane emissions from natural wetlands: 2. Interannual variations 1982–1993, Journal of Geophysical Research: Atmospheres, 106, 34207-34219, 10.1029/2001JD900164, 2001.

775 Warszawski, L., Frieler, K., Huber, V., Piontek, F., Serdeczny, O., and Schewe, J.: The Inter-Sectoral Impact Model Intercomparison Project (ISI–MIP): Project framework, Proceedings of the National Academy of Sciences, 111, 3228-3232, 10.1073/pnas.1312330110, 2014.

Watanabe, M., Chikira, M., Imada, Y., and Kimoto, M.: Convective Control of ENSO Simulated in MIROC, Journal of Climate, 24, 543-562, 10.1175/2010jcli3878.1, 2011.

780 Williams, M., Schwarz, P. A., Law, B. E., Irvine, J., and Kurpius, M. R.: An improved analysis of forest carbon dynamics using data assimilation, Global Change Biology, 11, 89-105, 10.1111/j.1365-2486.2004.00891.x, 2005.

Woodward, F. I., Smith, T. M., and Emanuel, W. R.: A global land primary productivity and phytogeography model, Global Biogeochemical Cycles, 9, 471-490, doi:10.1029/95GB02432, 1995.

Xenakis, G., and Williams, M.: Comparing microbial and chemical kinetics for modelling soil organic carbon decomposition using the DecoChem v1.0 and DecoBio v1.0 models, Geosci. Model Dev., 7, 1519-1533, 10.5194/gmd-7-1519-2014, 2014.

785 Zaehle, S., and Friend, A. D.: Carbon and nitrogen cycle dynamics in the O-CN land surface model: 1. Model description, site-scale evaluation, and sensitivity to parameter estimates, Global Biogeochemical Cycles, 24, doi:10.1029/2009GB003521, 2010.

Zhao, M., Heinsch, F. A., Nemani, R. R., and Running, S. W.: Improvements of the MODIS terrestrial gross and net primary production global data set, Remote Sensing of Environment, 95, 164-176, https://doi.org/10.1016/j.rse.2004.12.011, 2005.

790 Zhou, L., Tucker, C. J., Kaufmann, R. K., Slayback, D., Shabanov, N. V., and Myneni, R. B.: Variations in northern vegetation activity inferred from satellite data of vegetation index during 1981 to 1999, Journal of Geophysical Research: Atmospheres, 106, 20069-20083, 10.1029/2000JD000115, 2001.

Zona, D., Gioli, B., Commane, R., Lindaas, J., Wofsy, S. C., Miller, C. E., Dinardo, S. J., Dengel, S., Sweeney, C., Karion, A., Chang, R. Y.-W., Henderson, J. M., Murphy, P. C., Goodrich, J. P., Moreaux, V., Liljedahl, A., Watts, J. D., Kimball, J.
795 S., Lipson, D. A., and Oechel, W. C.: Cold season emissions dominate the Arctic tundra methane budget, Proceedings of the National Academy of Sciences, 113, 40-45, 10.1073/pnas.1516017113, 2016.

Earth System
Dynamics
Discussions
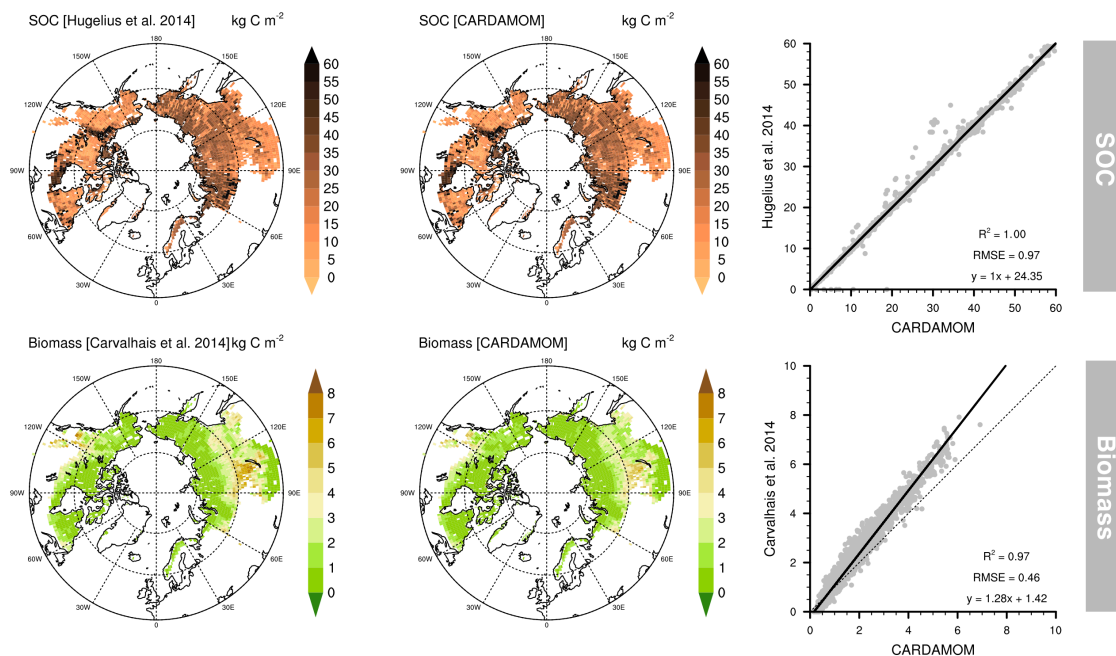
Figure 1. Original soil organic carbon [SOC; Hugelius et al., 2014] and biomass [Carvalhais et al., 2014] datasets used in the data assimilation process within the CARDAMOM framework (left hand side), assimilated SOC and biomass integrated in CARDAMOM (center), and their respective goodness-of-fit statistics between original and assimilated datasets (right hand side).

5
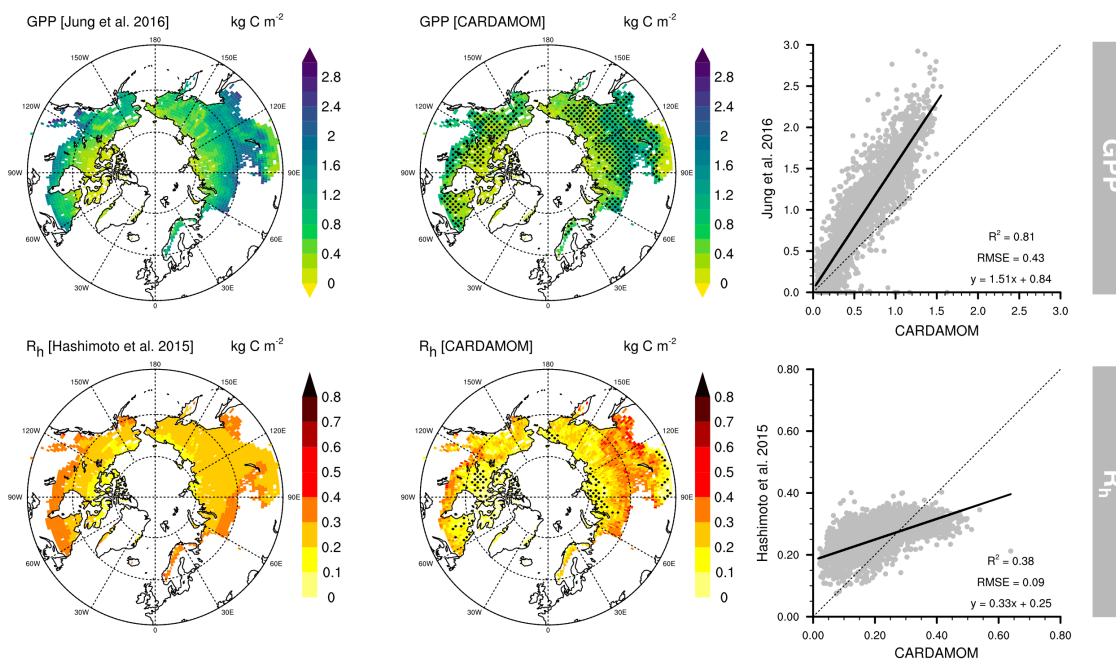
Figure 2. Original gross primary productitvity [GPP; Jung et al., 2016] and heterotropic respiration [R_h; Hashimoto et al., 2015] datasets used in the data validation process (left hand side), estimated GPP and R_h by CARDAMOM (center), and their respective goodness-of-fit statistics between original and assimilated datasets (right hand side). Stippling indicates locations where the

10 **independent datasets are within the CARDAMOM's 5th and 95th percentiles.**

Earth System
Dynamics

Discussions
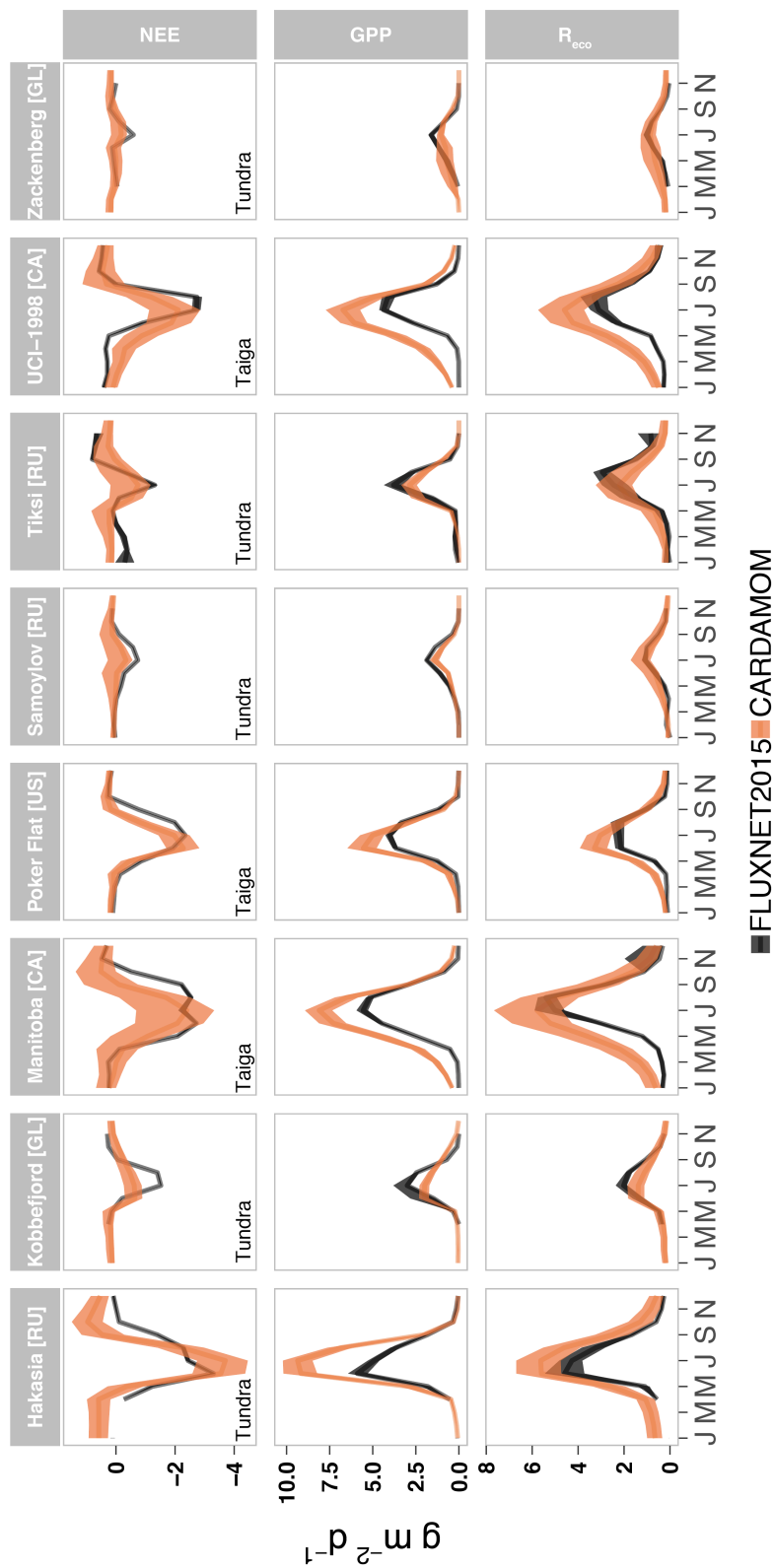
Figure 3. Monthly-aggregated seasonal variability of observed [FLUXNET2015] and modelled [CARDAMOM] C fluxes [NEE, Net Ecosystem Exchange; GPP, Gross Primary Production; R_{eco}, ecosystem Respiration] across eight low- and high-Arctic sites [Hakasia, Kobefjord, Manitoba, Poker Flat, Samoylov, Tiksi, UCI-1998 and Zackenberg]. Each of these sites, located in different countries [RU-Russia, GL-Greenland, CA-Canada, US-Unite States,] feature different meteorological conditions and vegetation types (Table S2). Uncertainties represent the 25th and 75th percentiles of both field observations and the CARDAMOM framework.
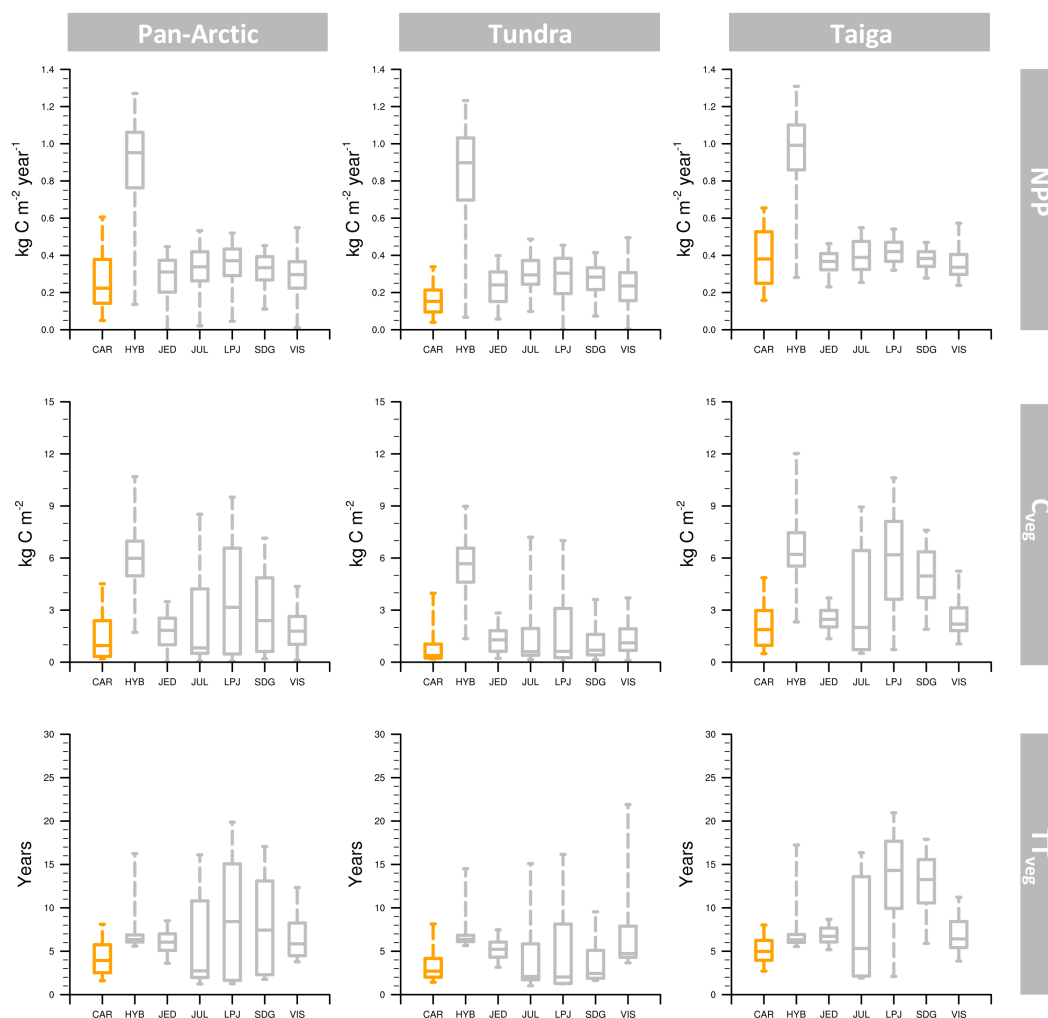
Figure 4. Central tendency and variability of NPP [Net Primary Production], C$_{veg}$ [Vegetation C pool], TT$_{veg}$ [Vegetation transit time] in the Pan-Arctic, tundra and taiga regions. The box whisker plots comprises the estimations between the 5th and 95th percentiles, and the box encompasses the 25th to 75th percentiles. The line in each box mark the median of studied variables in each region.

Earth System
Dynamics
Discussions
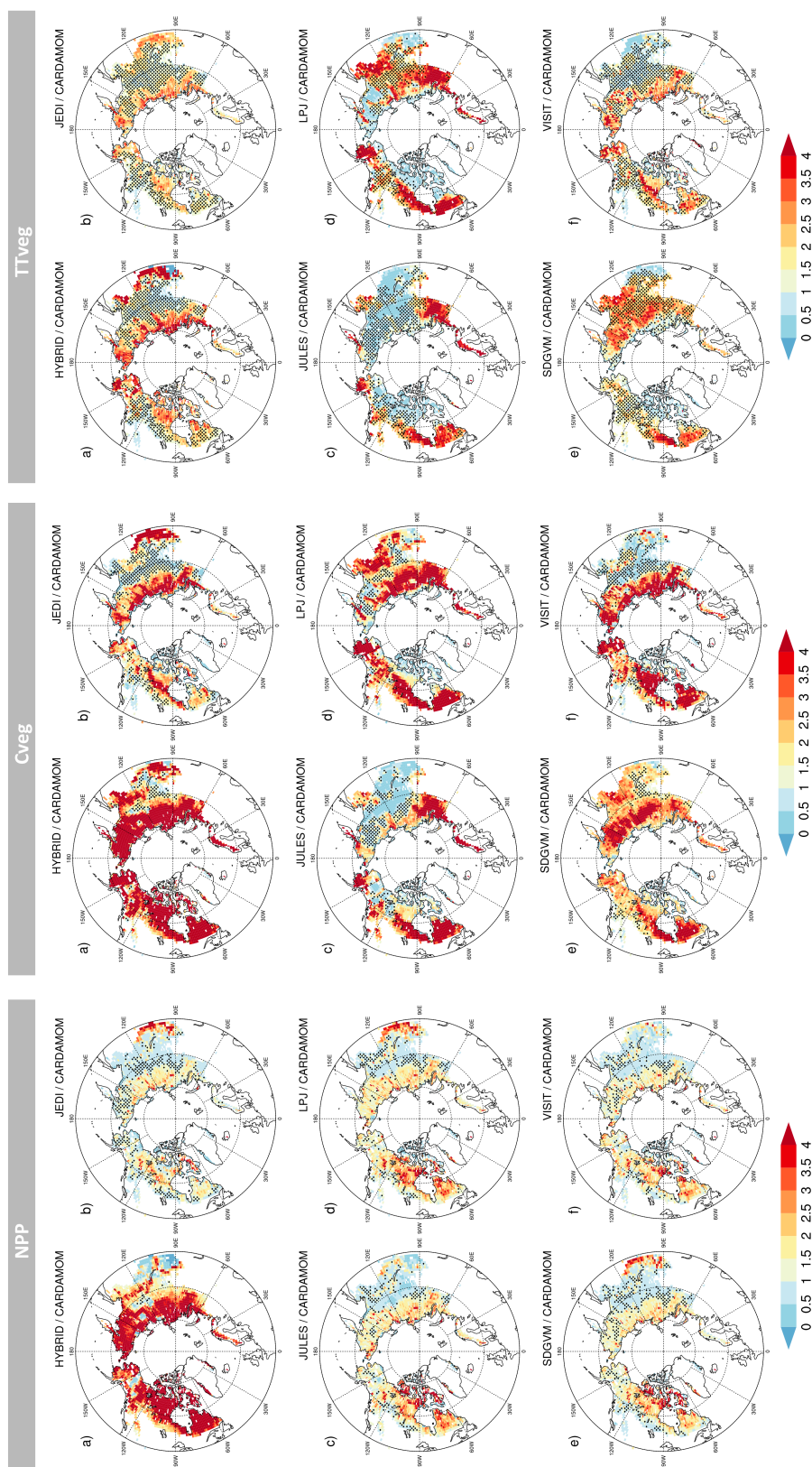
Figure 5. NPP [Net Primary Production], Cveg [Vegetation C pool] and TTveg [Vegetation transit time] ratios between ISI-MIP model ensembles [HYBRID, JEDI, JULES, LPJ, SDGVM and VISIT] and CARDAMOM. Stippling indicates locations where the ISI-MIP model mean is within the CARDAMOM's 5th and 95th percentiles.
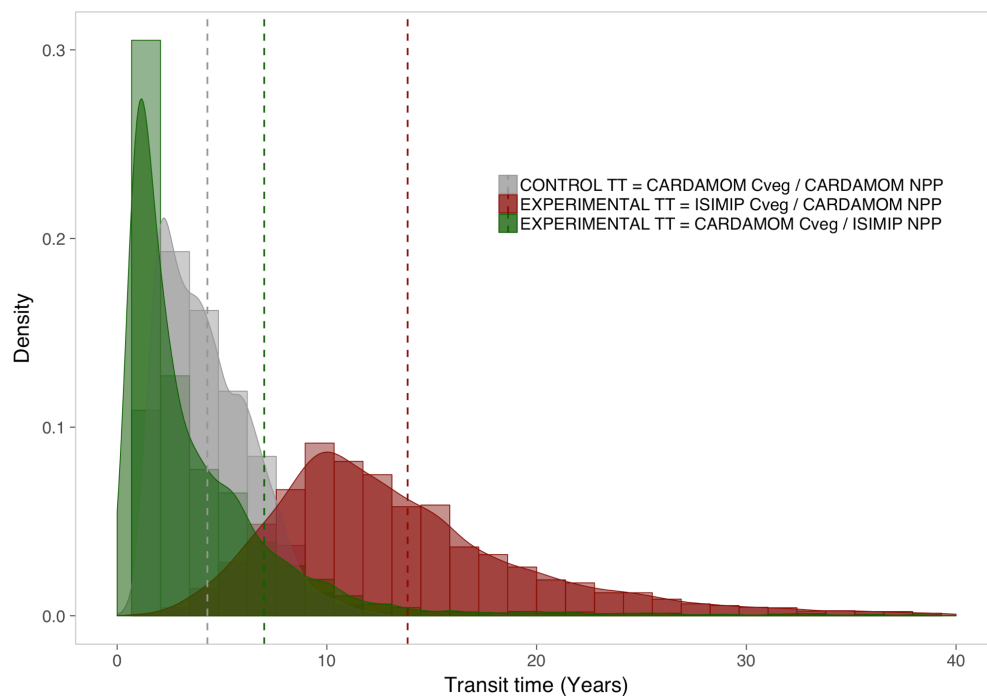
Figure 6. Distribution functions derived from the attribution analysis used to estimate the origin of vegetation transit time (TT$_{veg}$) bias from ISIMIP models. The control TT includes both biomass (C$_{veg}$) and net primary production (NPP) estimated by CARDAMOM (grey), while each of the two experimental TTs include C$_{veg}$ (yellow) and NPP (blue) from ISIMIP models. The lower the overlapped area is between control and experimental TT, the larger the contribution for TT biases is. Dashed lines represent the average TT value for each population. For readibility purposes, the scale in X-axis is delimited to 40 years.

Earth System Dynamics — Discussions — Open Access — EGU

Table 1. Multi-year (2000-2015) annual average of main ecosystem C fluxes [NEE, GPP, NPP, R_{eco}, R_a, R_h; g C m^{-2} yr^{-1}], C pools [C_{photo}, C_{veg}, C_{dom}, C_{tot}; kg C m^{-2}] and transit times [TT_{photo}, TT_{veg}, TT_{dom}, TT_{tot}; years] for the pan-Arctic, tundra (non-forested) and taiga (forested), region. The averages contain the estimations between the 5th and 95th percentiles, and the median in bold (50th percentile).

		Pan-Arctic					Tundra					Taiga				
		P05	P25	P50	P75	P95	P05	P25	P50	P75	P95	P05	P25	P50	P75	P95
C fluxes	NEE	-260.5	-152.0	**-55.8**	156.9	1158.1	-158.5	-81.1	**-13.0**	176.6	1107.7	-375.4	-232.0	**-104.1**	134.7	1215.0
	GPP	385.8	456.0	**513.1**	578.5	681.1	226.9	273.4	**315.0**	367.2	450.7	564.9	661.9	**736.5**	816.8	940.9
	NPP	177.4	224.6	**263.3**	307.3	376.6	104.8	133.9	**159.9**	192.1	243.9	259.3	326.9	**379.9**	437.1	526.1
	R_{eco}	193.2	316.3	**449.9**	716.6	1792.9	119.3	204.0	**300.0**	528.1	1515.0	276.6	442.9	**619.0**	929.1	2106.3
	R_a	164.3	207.7	**245.3**	289.9	364.0	98.4	126.5	**152.3**	184.9	239.9	238.7	299.2	**350.1**	408.2	503.9
	R_h	28.9	108.6	**204.6**	426.7	1428.9	21.0	77.5	**147.6**	343.2	1275.1	37.9	143.7	**268.9**	520.9	1602.3
C pools	C_{photo}	0.1	0.1	**0.1**	0.2	0.2	0.1	0.1	**0.1**	0.1	0.2	0.1	0.1	**0.2**	0.2	0.3
	C_{veg}	0.5	0.9	**1.4**	2.5	6.0	0.3	0.5	**0.8**	2.1	7.1	0.7	1.3	**2.0**	3.0	4.8
	C_{dom}	10.3	18.2	**24.4**	32.2	47.6	10.0	17.3	**23.3**	30.8	46.0	10.7	19.3	**25.7**	33.8	49.4
	C_{tot}	11.7	19.8	**26.2**	34.5	51.3	10.8	18.3	**24.6**	33.0	50.7	12.8	21.5	**28.0**	36.1	52.0
Transit times	TT_{photo}	0.9	1.1	**1.4**	1.7	2.2	1.0	1.3	**1.6**	2.0	2.8	0.7	0.9	**1.1**	1.3	1.6
	TT_{veg}	1.6	2.7	**4.3**	7.2	15.3	1.4	2.3	**3.5**	6.0	13.0	1.9	3.2	**5.2**	8.6	17.8
	TT_{dom}	10.2	54.5	**129.3**	266.0	891.1	11.3	63.1	**157.3**	329.9	1096.2	8.9	44.8	**97.9**	194.1	660.2
	TT_{tot}	11.9	59.9	**142.5**	297.8	1089.4	12.8	68.6	**173.1**	370.5	1347.4	10.8	50.0	**108.1**	216.2	800.1

Earth System
Dynamics
Discussions

Open Access

Table 2. Statistics of linear fit between the CARDAMOM framework (independent) and the FLUXNET2015 field observations (dependent) per individual site and per C flux [NEE, Net Ecosystem Exchange; GPP, Gross Primary Production; R_{eco}, ecosystem Respiration]. The units for RMSE and bias are g C m^{-2} month^{-1} in NEE, GPP and R_{eco}.

Flux	Site	Country	Intercept	Slope	R^2	RMSE	Bias
NEE	Hakasia	[RU]	0.89	1.40	0.85	0.67	0.49
	Kobbefjord	[GL]	-0.11	0.35	0.58	0.21	0.08
	Manitoba	[CA]	0.10	0.66	0.70	0.55	0.41
	Poker Flat	[US]	0.15	0.83	0.81	0.37	0.25
	Samoylov	[RU]	0.06	0.45	0.87	0.05	0.14
	Tiksi	[RU]	0.00	0.38	0.41	0.26	0.02
	UCI-1998	[CA]	-0.26	0.59	0.65	0.50	-0.15
	Zackenberg	[GL]	0.03	0.37	0.54	0.07	0.04
GPP	Hakasia	[RU]	-0.24	1.80	0.98	0.57	1.21
	Kobbefjord	[GL]	0.31	0.62	0.80	0.35	-0.07
	Manitoba	[CA]	0.63	1.30	0.93	0.73	1.15
	Poker Flat	[US]	0.06	1.20	0.93	0.51	0.30
	Samoylov	[RU]	0.01	0.70	0.98	0.06	-0.14
	Tiksi	[RU]	0.14	0.78	0.87	0.36	-0.05
	UCI-1998	[CA]	1.00	1.30	0.82	0.95	1.32
	Zackenberg	[GL]	0.22	0.57	0.84	0.14	-0.01
Reco	Hakasia	[RU]	0.59	1.20	0.98	0.30	0.87
	Kobbefjord	[GL]	0.12	0.65	0.86	0.17	-0.22
	Manitoba	[CA]	0.96	0.91	0.80	0.81	0.81
	Poker Flat	[US]	0.21	1.20	0.89	0.35	0.34
	Samoylov	[RU]	0.06	0.87	0.89	0.11	0.01
	Tiksi	[RU]	0.20	0.64	0.76	0.35	-0.15
	UCI-1998	[CA]	0.57	1.20	0.83	0.59	0.81
	Zackenberg	[GL]	0.24	0.66	0.86	0.09	0.10

Earth System Dynamics Discussions — Open Access — EGU

Table 3. Statistics of linear fit between the CARDAMOM framework (independent) and the ISIMIP models (dependent) per individual model and per NPP [Net Primary Production; kg C m⁻² yr⁻¹], C_{veg} [Vegetation C pool; kg C m⁻²] and TT_{veg} [Vegetation transit time; years]. The units for RMSE and bias are kg C m⁻² yr⁻¹ in NPP, kg C m⁻² yr⁻¹ [1] in C_{veg} and years in TT_{veg}.

| | | Panarctic | | | | | Tundra | | | | | Taiga | | | | |
		Slope	Intercept	R^2	RMSE	Bias	Slope	Intercept	R^2	RMSE	Bias	Slope	Intercept	R^2	RMSE	Bias
NPP	HYBRID	0.80	0.30	0.03	0.30	0.61	0.66	1.00	0.09	0.30	0.66	1.00	-0.21	0.01	0.28	0.55
	JEDI	0.17	0.44	0.48	0.08	0.02	0.13	0.59	0.29	0.09	0.06	0.26	0.25	0.35	0.05	-0.03
	JULES	0.25	0.36	0.29	0.10	0.07	0.19	0.68	0.33	0.09	0.13	0.33	0.17	0.09	0.09	0.00
	LPJ	0.22	0.48	0.41	0.10	0.08	0.15	0.78	0.31	0.11	0.11	0.35	0.20	0.21	0.06	0.03
	SDGVM	0.21	0.41	0.52	0.07	0.05	0.17	0.60	0.35	0.08	0.11	0.28	0.26	0.47	0.04	-0.01
	VISIT	0.18	0.43	0.28	0.12	0.02	0.11	0.80	0.28	0.12	0.07	0.30	0.17	0.07	0.10	-0.03
C_{veg}	HYBRID	5.90	0.13	0.00	2.90	4.61	5.60	-0.05	0.00	2.40	4.60	6.80	-0.01	0.00	3.20	4.62
	JEDI	1.40	0.32	0.24	0.84	0.41	1.30	0.00	0.00	0.80	0.45	1.80	0.32	0.40	0.54	0.37
	JULES	1.80	0.55	0.08	2.80	1.07	1.60	0.15	0.01	2.40	0.85	2.20	0.57	0.07	3.00	1.30
	LPJ	2.40	0.88	0.15	3.10	2.26	1.90	0.06	0.00	2.40	0.92	4.20	0.79	0.13	2.80	3.77
	SDGVM	1.60	0.91	0.31	2.00	1.45	1.10	0.07	0.01	1.10	0.21	3.10	0.86	0.44	1.30	2.81
	VISIT	1.70	0.17	0.03	1.40	0.45	1.50	-0.06	0.00	1.20	0.45	2.40	0.10	0.01	1.30	0.44
TT_{veg}	HYBRID	8.70	-0.07	0.00	13.00	4.14	8.80	-0.01	0.00	15.00	5.25	8.10	-0.01	0.00	10.00	2.91
	JEDI	4.80	0.29	0.18	1.30	1.80	5.00	0.07	0.01	1.30	1.93	5.40	0.29	0.19	0.97	1.67
	JULES	4.00	0.46	0.03	5.30	1.76	4.40	0.07	0.00	4.70	1.19	5.20	0.46	0.02	5.50	2.36
	LPJ	4.80	0.97	0.10	6.40	4.70	5.10	0.03	0.00	5.20	1.63	9.00	0.84	0.06	5.50	8.16
	SDGVM	2.70	1.30	0.24	4.80	3.81	3.20	0.18	0.02	2.70	0.34	6.60	1.20	0.32	3.00	7.64
	VISIT	3.00	1.40	0.01	31.00	4.85	-0.20	3.20	0.03	43.00	7.60	7.20	-0.05	0.00	2.30	1.80